We are IntechOpen, the world's leading publisher of Open Access books Built by scientists, for scientists

4,800
Open access books available

122,000
International authors and editors

135M
Downloads

Our authors are among the

154
Countries delivered to

TOP 1%
most cited scientists

12.2%
Contributors from top 500 universities

CLARIVATE ANALYTICS BOOK CITATION INDEX INDEXED

WEB OF SCIENCE™

Selection of our books indexed in the Book Citation Index in Web of Science™ Core Collection (BKCI)

Interested in publishing with us?
Contact book.department@intechopen.com

Numbers displayed above are based on latest data collected.
For more information visit www.intechopen.com

1

Solar Nanocomposite Materials

Zhengdong Cheng
Artie McFerrin Department of Chemical Engineering
And the Materials Science and Engineering program
And the Professional Program in Biotechnology
Texas A&M University, College Station, Texas
USA

1. Introduction

The energy from the sun that strikes the earth is a gigantic 3×10^{24}J a year, or about 10,000 times more than what the global population currently consumes (M. Gratzel, 2007; B. Li, et al., 2006). World energy consumption is 5.0×10^{20}J and is expected to grow about 2% each year for the next 25 years (Us_Energy_Information_Administration, 2010). Covering 0.1% of the earth's surface with solar cells at an efficiency of 10% would provide the current energy needs of the whole world (B. Li, et al., 2006). However, the electricity generated from solar cells today is less than 0.1% of the world's total energy demand (P. V. Kamat, 2007). The first generation photovoltaic devices (PV) are based on single- or multi-crystalline p-n junction silicon cells. They are commercially available for installation with market share of about 85% and deliver power with 15% efficiency, but suffer from high cost of manufacturing and installation. There are high purity requirements for the silicon crystals, high fabrication temperatures and a large amount of material is needed for a wafer-based cell. The second generation PV devices use polycrystalline semiconductor thin films, mostly based on CdTe, having a market share of 15% (S. Ruhle, et al., 2010). Thin films of $CuInGaSe_2$ (CIGS) bring down the cost but their efficiency needs to improve for practical applications. The third generation devices will be based on nanocomposites (nano-structured semiconductors, organic-inorganic hybrid assemblies, and molecular assemblies), aiming to deliver high efficiency at an economically viable cost (P. V. Kamat, 2007). Nanostructure offers spatial quantum confinement for the tailor of the optical properties of semiconductor nanomaterials. The use of multi-components offers a high degree of flexibility for altering and controlling properties and functionalities of nanocomposites.

Nanocomposites are developed for superior device performance. In solar energy harvest and conversion, nanocomposites are utilized to overcome limits of single materials in solar spectrum response (band gap engineering), transport of electrons or holes (defect engineering), reaction of electrons or holes with chemicals (catalyst engineering), and reduce of costs (economic consideration).

2. History of solar nanocomposites

The first modern PV solar cells, silicon (Si) p/n, were developed by Chapin *et al.* at Bell laboratories in 1954 (D. M. Chapin, et al., 1954). These so called *first generation solar cells* cost

about $4/W due to the materials used (the high quality and low defect single crystal Si, the strengthened low-iron glass cover sheet, and encapsulants). They are quickly used in space exploration. Considerable domestic use begun in 1978 when NASA installed a 3.5 kW system in a 16-home India village in Papago reservation, Arizona. Apart from regular use in power calculator, traffic signs, clocks and other small appliances, the use of solar cells has grow slowly although steadily (L. M. Goncalves, et al., 2008). The first amorphous Si cell (a-Si) appeared in 1976 right after the first oil shock (D. E. Carlson & C. R. Wronski, 1976). The high absorption rate of a-Si comparing to crystal silicon make it be a thin film technology. The thin film technology based solar cells are often called the *second generation solar cells*. They aimed at lower cost than the first generation. Among the three thin film technologies (a-Si, CdTe and $Cu(In,Ga)Se_2$), $Cu(In,Ga)Se_2$ (CIGS) cells have the best future due to higher efficiencies, confirmed maximum efficiency of 19.2% in 1999 (M. A. Contreras, et al., 1999; M. A. Green, et al., 2008) and low manufacturing energy consumption. Both first and second generation solar cells are based on single junction devices, for which the calculated thermodynamic efficiency limits (33.7%) is called Shockley-Queisser limit (W. Shockley & H. J. Queisser, 1961). Six junction (6J) cell (AlInGaP/InGaP/AlInGaAs/InGaAs/InGaNAs/Ge) has a predicted maximum efficiency of 57% (M. Bosi & C. Pelosi, 2007). A theoretical limit for infinity-layer cell is 68% (A. Devos, 1980). In space applications where cost is not the major problem, multi-junction cells have replaced Si cells. The second generation solar cells and multi-layer semiconductor stack cells are still under development.

1883	Vogel	Ag-dye
1954	Chapin *et al.*	Si-p/n
1972	Fujishima &Hoda	TiO_2 water splitting
1976	Carlson *et al.*	a-Si
1976	Matsumura *et al.*	ZnO-DSSC
1984	Serpone *et al.*	QDSSC
1991	Gratzel *et al.*	TiO_2-DSSC
1999	Contreras *et al.*	CIGS 19% efficiency

Table 1. History of solar nanocomposites

Historically, photographic films were particularly insensitive to mid-spectrum and red light due to wide band gap of the silver halide grains range from 2.7 eV to 3.2 eV (**Fig.1**) which has negligible absorption at wavelengths longer than 460nm (M. Gratzel, 2001). In 1883, Vogel discovered (W. West, 1974) that silver halide emulsion could be sensitized by adding a dye to extend the photosensitivity to longer wavelength. Four years later, this concept of dye enhancement was carried over to photoelectrochemistry cells by Moser using erythrosine on silver halide electrodes (M. Gratzel, 2001). It was later recognized that that the dye should be adsorbed on the semiconductor electrodes in a closely packed monolayer for maximum efficiency (R. C. Nelson, 1965), and electron transfer to be the prevalent

mechanism for the sensitization (K. Hauffe, et al., 1970). Photoelectrochemistry became a thriving research field on the foundation laid down by the work of Brattain and Garret (W. H. Brattain & C. G. B. Garrett, 1955) and subsequently Gerischer (H. Gerische, 1966) who took the first detailed electrochemical and photochemical studies of the semiconductor-electrolyte interface.

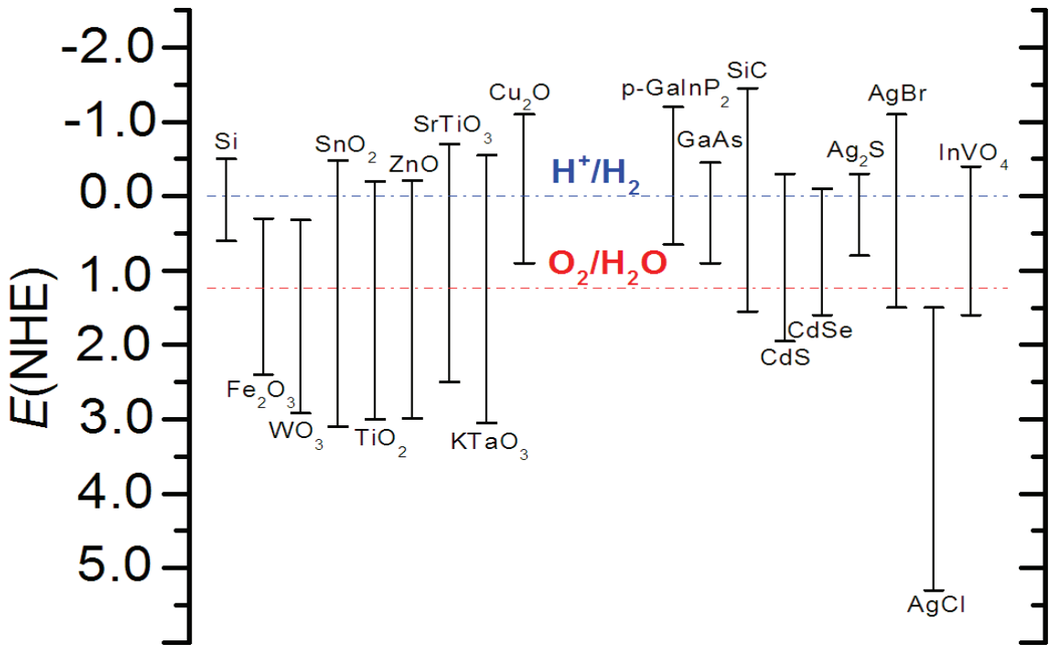

Fig. 1. Band gaps of semiconductors.

The oil crisis in 1973 fueled a rapid research on photoelectrochemical cells (K. Kalyanasundaram, 1985). TiO_2 became the favored semiconductor for water photolysis following its use by Fujishima and Honda in 1972 (A. Fujishima & K. Honda, 1972). The solution to the problem that narrow-bangap semiconductors for efficient absorption of sunlight are unstable against photo-corrosion came in the separation of optical absorption and charge-generating functions. An electron transfer sensitizer is used to absorb the visible light and inject charge carriers across the semiconductor-electrolyte junction into a substrate with a wide bandgap, which is stable. This concept leads to the development of *dye-sensitized solar cells* (DSSC) in 1991 (B. Oregan & M. Gratzel, 1991) (Matsumura *et al.* developed ZnO-DSSC in 1976 (H. Tsubomura, et al., 1976)). In DSSC, the semiconductor is in the *mesoscopic* state (M. Gratzel, 2001): minutely structured with an enormous internal surface area (percolating nanoporous networks). The semiconductor (TiO_2, ZnO, SnO_2, CdSe etc.) films are made up of arrays of tinny crystals measuring a few nanometers across, which are interconnected to allow electronic conduction to take place. This structure has a much larger surface area (over a thousand times) available for dye chemisoprtion than a flat, unstructured electrode. The photocurrent in standard sunlight increased 10^3-10^4 times when passing from a single crystal to a nano-crystalline electrode. A overall power conversion efficiency of 10.4% has been obtained for DSSC (M. A. Green, et al., 2008; M. K. Nazeeruddin, et al., 2001). The record efficiency of DSSC is 12% for small cells and about 9% minimodules (A. Hagfeldt, et al., 2010).

The successful of DSSC has rekindled interest in tandem cells for water splitting by visible light. Tandem cells are needed for two reasons. First, most metal oxide semiconductors (such as WO_3, Fe_2O_3 and TiO_2) can only reduce or oxidize water, not both. Secondly, most of the oxide semiconductors only absorb UV light. With DSSC can efficiently utilize the visible light and TiO_2 can reduce water, TiO_2 DSSC are used as bottom electrode to absorb the visible light and reduce water to hydrogen gas, which is in couple to the top electrode, either crystalline WO_3 (C. Santato, et al., 2001) or Fe_2O_3 (S. U. M. Khan & J. Akikusa, 1999) to absorb the blue part of the sunlight. This configuration is in close analogy to the "Z-scheme" of the photosynthesis of the green plants adsorbing complementary parts of the solar spectrum, where one photosystem oxidizes water to oxygen and the other generate the compound NADPH used in fixation of carbon dioxide. At present, the overall conversion efficiency from standard solar light to chemical energy is 4.5%.

Further the idea of sensitization, but using quantum dots (QDs) instead of dye to be attached to the semiconductor oxide matrix as light absorbers, we see the birth of the quantum dots sensitized solar cells (QDSCs) in 1984 (N. Serpone, et al., 1984). Comparing to DSSC, QDSSC has higher absorption, greater stability, wider tunable responsible wavelength range, and importantly the possibility to exploit *multiple exciton* generation and utilize *hot electrons* whose energy is higher than the low limit of conduction band (A. J. Nozik, 2002). The solar efficiency of liquid junction QDSSCs has reach 4.9% at present (G. Hodes, 2008; Q. X. Zhang, et al., 2011). The name of the *third generation solar cells* are given to devices (M. A. Green, 2003) aim to overcome the Shockley-Queisser limit of single junction or single band gap devices (33.7%), even the limit of an infinite stack of band gaps that perfectly matched to the solar spectrum (68%), and large-scale implementation. In principle, sunlight can be converted to electricity at efficiency close to Carnot limit of 93%. QDSSCs are very promising third generation solar cells due to their potential of achieving competitive cost-efficiency ratio. DSSCs are second generation solar cells with the possibility to become third generation devices if the efficiency can be largely improved.

3. PV cells

3.1 Dye Sensitized Solar Cells

DSSCs differ from conventional semiconductor devices in that they separate the function of light absorption from charge carrier transport, which solves the instability problem of narrow bandgap semiconductors using the concept very close to compositing. Dye sensitizer absorbs the incident sunlight (**Fig.2** (M. Gratzel, 2004)) and exploits the light energy to induce vectorial electron transfer reaction. DSSC has the following advantages comparing with the Si based photovoltaics (D. Wei, 2010). (1) It is not sensitive to the defects in semiconductors such as defects in Si. It was found that the charge transport of photo-generated electrons passing the nanocrystalline particles and grain boundaries is highly efficient (U. Wurfel, et al., 2008). (2) The semiconductor-electrolyte interface (SEI) is easy to form and it is cost effective for production. (3) It is possible to realize the direct energy transfer from photons to chemical energy using nanoporous structures that offer a enormous surface area (1000 fold enhancement comparing a monolyer) for the adsorption of dye molecules. Other names for DSSC are dye-sensitized nanostructured solar cells, mesoscopic injection solar cells, nanosolar cells, the artificial leaves, or Gratzel cells (A. Hagfeldt, et al., 2010). (4) It is a *cheaper* alternative to silicon solar cells.

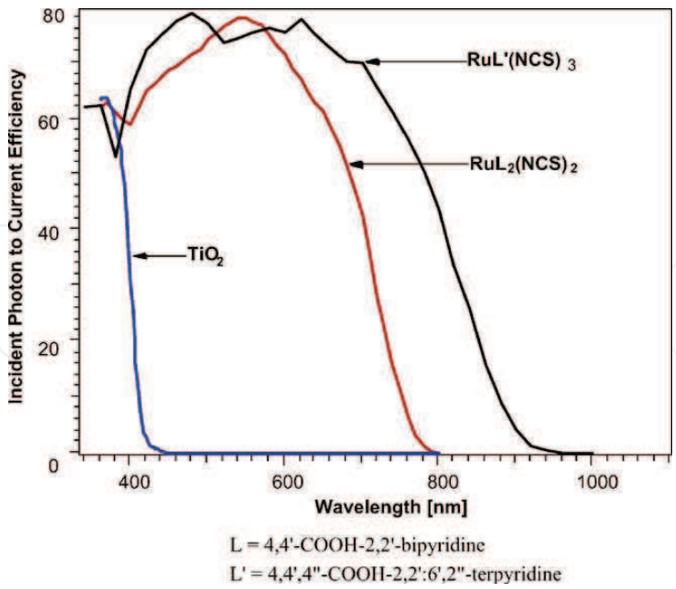

Fig. 2. Sensitization effect. DSSCs can convert visible light into electricity while TiO_2 only cannot.

Because of the encapsulation problem posed by liquid in the conventional wet DSSC, much work has also been done on an all solid DSSC (U. Bach, et al., 1998). To construct a full solid-state DSSC, a solid p-type conductor should be chosen to replace the liquid electrolyte. The redox levels of the dye and p-type materials have to be adapted carefully to result in an electron in the conduction band of n-type semiconductors (e.g., TiO_2, ZnO (H. Tsubomura, et al., 1976), SnO_2, $SrTiO_3$) and a hole localized on the p-type conductor (e.g., CuI (K. Tennakone, et al., 1998), CuSCN (B. Oregan & D. T. Schwartz, 1995)). Solid DSSC has also been fabricated using TiO_2 and conducting *polymers* (polypyrrole (K. Murakoshi, et al., 1998) and polyaniline (S. Ameen, et al., 2009)) and low bandgap polymer (W. S. Shin, et al., 2007). Solid state DSSCs based on ionic liquids were also reported to enhance the conversion efficiency (P. Wang, et al., 2003), and the non-volatile character of ionic liquids offers the easy packaging for printable DSSCs.

Plastic and solid state DSSCs incorporating single walled carbon nanotubes (SWNT) have been fabricated (N. Ikeda & T. Miyasaka, 2007). When employing SWNT as conducting scaffolds in a TiO_2 based DSSC, the photoconversion efficiency can be boosted by a factor of 2 (A. Kongkanand, et al., 2007). Graphene was also introduced to the study of DSSC recently. Transparent, conductive and ultrathin graphene films are used as an alternative to the ubiquitously employed metal oxides window electrodes in DSSCs (X. Wang, et al., 2008). In terms of publications, ZnO is so far the runner up to TiO_2, mainly attributed to the relative ease of synthesizing highly crystalline ZnO with various morphologies, such as nanoparticles, nanowires, nanorods, nanotubes, tetrapods, nanoflowers, nanosheets and branched nanostructures. Nanostructured ZnO has been synthesized via a wide range of techniques. Historically, ZnO was one of the first semiconductors used in DSSCs (H. Tsubomura, et al., 1976). The band gap of ZnO is similar to TiO_2 (**Fig.1**). ZnO has higher electron mobility than TiO_2, which should favor electron transport. However, ZnO is not chemically stable; it dissolves under both acidic and basic conditions. Other metal oxides used in DSSCs include SnO_2, $SrTiO_3$ and others.

DSSC is the only solar cell that can offer both flexibility and transparency. Solid state and printable DSSCs will have a promising future for the development of efficient and flexible optoelectronics (S. Gunes & N. S. Sariciftci, 2008). Their efficiency is comparable to amorphous silicon solar cells but with a much lower cost, longer lasting and work at wide angles. Also, DSCCs work more efficiently in indoor light because dye absorbs diffuse sunlight and fluorescent lighting (D. Wei, 2010).

A challenging but realizable *goal* for the present DSSC technology is to achieve efficiencies above 15%. It requires developing dye-electrolyte systems that give efficient regeneration of the oxidized dye at a driving force of 0.2-0.4 V (A. Hagfeldt, et al., 2010). DSSCis a good example of a system where the function of the overall device is better than predicted from the sum of the properties of its components (A. Hagfeldt, et al., 2010). The nanostructured TiO_2 electrode does not conduct any electrical current and itself is a very good insulator. The conventional N3 dye dissolved in a solution degrades after a few hours under light. But when these are brought together in a well-working device, the solar cell conducts electrical current up to 20 mA/cm^2 and the dye will stable for more than 15 years in outdoor solar radiation. Therefore, the photovoltaic function is the emergent property of the device that is made of the individual entities of the semiconductor, the sensitizer and the electrolytes.

The future directions for the development of DSSCs include (1) organic dyes that can extend light absorption into the near infrared with good photo and thermal stability (K. Kalyanasundaram & M. Gratzel, 1998), (2) synthesis and modification of various type of TiO_2, or other semiconductors, nanomaterials (X. B. Chen & S. S. Mao, 2006), and (3) modification of the physical properties of TiO_2 nanostructures to extend optical absorption into the visible region (X. B. Chen, et al., 2005; S. U. M. Khan, et al., 2002).

3.2 Quantum Dots Sensitized Solar Cells

The concept of Quantum dot (QD) sensitized solar cells (QDSSCs) is borrowed from the photoelectrochemical Gratzel's cells, the dye sensitized solar cells (DSSC) (B. Oregan & M. Gratzel, 1991). Due to the similar size of QDs and the nanocrystals of the metal oxide semiconductors, *all QDSSCs are nanocomposites* in tend to optimize the solar spectrum response of the resulted materials.

Quantum dot sensitizers for solar cells have several promising advantages over dye sensitizers: (1) Tunable energy gaps (S. Gorer & G. Hodes, 1994). The band gaps can be simply adjusted by changing the size and shape of QDs, and well match the solar spectrum. Also, there is a wider band gap range of semiconductor than dyes. (2) Large absorption coefficient (typically by a factor of 5 (G. Hodes, 2008)) (I. Moreels, et al., 2007). The high extinction property of bulk semiconductors are preserved at the nanoscale (W. W. Yu, et al., 2003). (3) Multiple electro-hole pair production per photon utilizing hot electrons (V. I. Klimov, 2006; A. J. Nozik, 2002; R. D. Schaller & V. I. Klimov, 2004; Y. Takeda & T. Motohiro). Other advantages include superior resistance towards photobleaching over organometallic or organic dyes (G. Hodes, 2008), low cost and easy to synthesis. In addition, the production of QDs is significantly cheaper compared to their bulk counterparts since their synthesis takes place at significantly lower temperatures and with solution-based approaches.

In spite of the above advantages of QDs compared with dyes, the best reported efficiencies of QDSSCs are still lower than that of DSSCs. Large improvement in efficiency of QDSSCs, comparable to DSSCs, is expected. The main differences between these two type of solar

cells are (G. Hodes, 2008) : (1) Multiple layer absorption of QDs on the mesoporous oxide surface compared to a monolyer of absorbed dye might hindrance the electron transfer rate from the QD to the oxide. (2) Different electrolytes are used (I. Mora-Sero & J. Bisquert, 2010). The polyiodide electrolyte used in DSSC might be also beneficial to QDSSC. However, the choice of electrolyte will depend on the specific adsorbing semiconductor used, and no optimized electrolyte system has been obtained. (3) The presence of considerable surface charge traps on absorbed QDs which increases recombination. Passivation of surface states on the QDs can be done, after deposition of the QDs to the oxide, by coating the QDs with suitable band-aligned semiconductor shell or by adsorbing long chain organic passiviting molecules onto the QDs. Passivation of the QD-Oxide interface might be pre-deposition of a buffer layer or small molecules on the oxide before QD deposition. Wide band gap semiconductor ZnS has coated on the surface of CdS QDs that were *grown* in situ on TiO_2 inverse opal and led to a higher efficiency due to the decrease of QD surface traps (L. J. Diguna, et al., 2007b).

A recent study presented CdS QDSSC based on a mesoporous TiO_2 film with remarkable stability using I^-/I_3^- electrolyte (M. Shalom, S. Dor, et al., 2009). Chemical Bath Deposition (CBD) was used to *deposit* the CdS QDs within the porous network. A thin coating of the QD sensitized film with an *amorphous TiO_2 layer* has improved the performance and photo-stability of the solar cell, which confirmed the hypothesis that the coating passivates QD surface states which act as hole traps and are responsible for photodegradation of the device. In addition, this coating decreased the recombination of electrons from the CdS QDs and the mesoporous TiO_2 into the electrolyte solution. A total light to electric power conversion efficiency of 1.24% was achieved.

The conduction and valence bands levels of QDs play an important role in dictating capture of photogenerated electrons and holes at the interface. Both CdSe and CdTe QDs bind strongly to TiO_2 through a linker molecule, and inject electrons into TiO_2 with an ultrafast rate under bandgap excitation. CdTe has a more negative conduction band (-1.25V vs NHE, normal hydrogen electrode) compared to CdSe (-1.2V vs NHE) and hence injects electrons into TiO_2 nanoparticles at a faster rate. The reactivity of photogenerated holes with the sulfide electrolyte, however, determines their suitability in QDSSCs (J. H. Bang & P. V. Kamat, 2009). CdSe remains regenerative during the operation of QDSSC as the photogenerated holes are scavenged by S^{2-} ions. A maximum Incident Photo to Charge conversion efficiency (IPCE) of 70% shows the suitability of this system in a photoelectrochemical solar cell. The scenario is, however, different for CdTe-based QDSC. The formation of a CdS shell and the inability to scavenge photogenerated holes make CdTe a poor candidate for QDSCs. A series of other redox couples were used in the photoelectrochemical cells as a replacement of the S^{2-}/S_n^{2-} , none of them seems to provide the required photostability for the CdTe QD electrodes; most of them immediately corrode CdTe QDs even under ambient conditions. Despite the fast electron injection rate was observed, it has a poor external quantum efficiency (3%) (J. H. Bang & P. V. Kamat, 2009). The difference in the performance of these two systems has been understood based on the position of their valence bands (0.53V in CdSe and 0.1V in CdTe). The energy levels of valence bands are such that redox couples such as a sulfide/polysulfide couple (-0.5V) scavenge holes only from CdSe and *not* from CdTe. This failure to scavenge photogenerated holes results in the degradation of CdTe. Hence, the choice of CdTe for the operation of QDSSCs (*i.e.*, photoelectrochemical cells) currently poses a serious challenge.

There are generally two methods are adopted to realize QDs sensitizers over mesoporous TiO_2 films: (1) direct growth of the QDs on the TiO_2 photoanode surface by chemical bath deposition (CBD) or by successive ionic layer adsorption and reaction (SILAR); (2) pre-synthesized colloidal QDs attached to the electrode surface directly or with the aid of bifunctional linker molecules. These methods sometimes are combined in order to achieve co-sensitized deposition (L. Yin & C. Ye, 2011; Q. X. Zhang, et al., 2011). For example, CdSe can be pre-synthesized in a colloidal form with different shapes and sizes that may be directly attached to the wide band gap semiconductors (the electron-transport matrix) (S. Gimenez, et al., 2009; N. Guijarro, et al., 2009) or through bifunctional linker molecules (H. J. Lee, et al., 2008; I. Mora-Sero, et al., 2008; I. Robel, et al., 2006). It has also been directly grown on the surface on a wide gap semiconductor by CBD (L. J. Diguna, et al., 2007a; O. Niitsoo, et al., 2006; Q. Shen, et al., 2008), SILAR (H. Lee, et al., 2009) or electrodeposition (C. Levy-Clement, et al., 2005).

In QDSSC, the diameter of QDs anchored on the photoanode generally ranges from 3 to 8 nm, much larger than that of dyes. For the normal nanoparticle-based TiO_2 film, its inner pores are much easier to be blocked while depositing QDs. Other factors such as TiO_2 morphology, surface area, inner pore structure etc. will strongly influence the QDs loading and cell performance. Of course, optical confinement and light scattering effect to improve the light absorption efficiency are also necessary. Aiming at improving the efficient assembly of the QDs onto the TiO_2 photoanode, the influence of structural properties of various TiO_2 photoanodes on the photovoltaic performance of CdS/CdSe- QDSSCs has been systematically investigated (Q. X. Zhang, et al., 2011). The results revealed that unlike conventional DSSCs, the main contribution of the scattering layer to QDSSCs is adjusting the aperture distribution of TiO_2 working electrode for CdS/CdSe deposition, extending the light path length and decreasing the electron recombination. In the meantime, an introduction of large size 300 nm TiO_2 particles into the photoanode can achieve a wider pore size distribution from several nanometers to over 50 nanometers for effective CdS/CdSe coverage on the surface of TiO_2 photoanodes as well as facilitating the polysulfide electrolyte penetration in the TiO_2 films. A double-layer photoanodic structure can gave 4.92% of light-to-electricity conversion efficiency with 0.15 cm^2 of photoactive area, which is among the best results for the QDSSCs.

To harvest as much as possible the solar energy, combination of the absorber materials with varied band gap (*nanocomposite absorbers*) have been tested (V. Gonzalez-Pedro, et al., 2010; Y. L. Lee & Y. S. Lo, 2009; O. Niitsoo, et al., 2006). An interesting study shows that CdS and CdSe QDs have a complementary effect in light harvesting and the performance of a QDs co-sensitized solar cell is strongly dependent on the order of CdS and CdSe respected to the TiO_2 (**Fig.3 a&b**. TiO_2/CdS(3)/CdSe(4) means TiO_2 nanoporous film was deposited CdS QDs by 3 CBD cycles followed by deposition of CdSe by 4 CBD cycles) (Y. L. Lee & Y. S. Lo, 2009). In the cascade structure of TiO_2/CdS/CdSe electrode, the re-organization of energy levels (**Fig.3c**) between CdS and CdSe forms a stepwise structure of band-edge levels which is advantageous to the electron injection and hole-recovery of CdS and CdSe QDs. An energy conversion efficiency of 4.22% is achieved using a TiO_2/CdS/CdSe/ZnS electrode, under the illumination of one sun (AM1.5, 100 mW cm^{-2}). The present of CdS between TiO_2 and CdSe does not inhibit the transport of excited electron from CdSe to TiO_2, but it is not the case when you switch CdS and CdSe. In the long-wavelength region where only CdSe can be photoexcited, the IPCE increment of the TiO_2/CdS/CdSe device, with respect to that

of TiO_2/CdSe, indicates that the presence of CdS between TiO_2 and CdSe should take the responsibility for the performance enhancement of the TiO_2/CdS/CdSe device (**Fig.3b**).

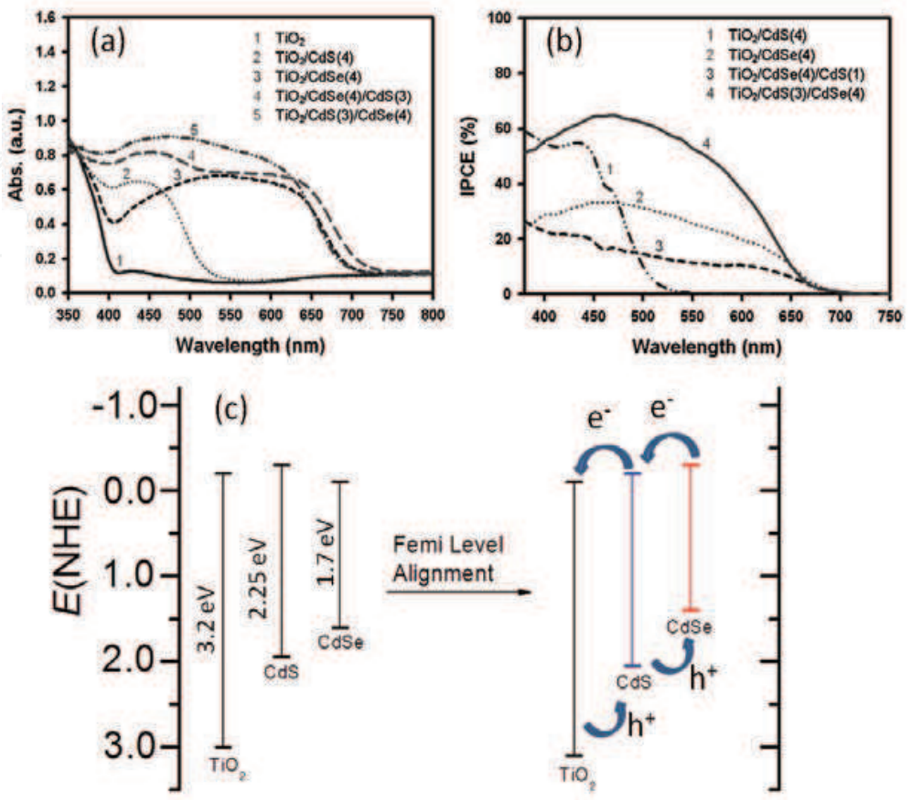

Fig. 3. Femi level alignment.

That is, the presence of CdS is helpful to the collection of excited electrons from CdSe to TiO_2, which takes major contribution to the cosensitization effect of the TiO_2/CdS/CdSe device. On the other hand, when CdS is deposited on TiO_2/CdSe, the IPCE of the TiO_2/CdSe/CdS device is lower than that of TiO_2/CdSe and TiO_2/CdS devices, which means that introduction a CdSe layer between TiO_2 and CdS is detrimental to the transport of excitons and, therefore, the co-sensitization effect cannot be achieved. The band edges of TiO_2, CdS, and CdSe in bulk are schematically shown in **Fig.3c**. When CdS and CdSe were brought in contact as a cascade structure, the energy levels difference (Fermi level difference if they follow Fermi–Dirac statistic) between CdS and CdSe causes the electrons flow from CdS (higher level) to CdSe (lower level). Such electron transfer is known as the *Fermi level alignment* if the material can be described by Fermi-Dirac distribution. The redistribution of the electrons between CdS and CdSe is supposed to trigger a downward and upward shift of the band edges, respectively, for CdS and CdSe. Therefore, the resulting band edges for the TiO_2/CdS/CdSe device are inferred to have a stepwise structure as shown in **Fig.3c**. Both the conduction and valence bands edges of the three materials increase in the order: TiO_2<CdS<CdSe. That is, the insertion of a CdS layer between TiO_2 and CdSe elevates the conduction band edge of CdSe, giving a higher driving force for the injection of excited electrons out of CdSe layer. This is why a higher IPCE was obtained for the TiO_2/CdS/CdSe

device in the long-wavelength region, compared with the TiO_2/CdSe device. When both CdS and CdSe are photoexcited under white light illumination, the stepwise structure of the band edges is advantageous not only to the electron injection but also to the hole-recovery for both the inner CdS and outer CdSe layers. On the contrary, in the TiO_2/ CdSe/CdS device, the conduction and valence bands edges of intermediate CdSe will be higher respected to those of CdS. In such an energy structure, energy barriers exist for injecting an excited electron from outer CdS layer and transferring a hole out of inner CdSe, which causes a low IPCE of the TiO_2/CdSe/CdS device.

It is possible to design both injection and recombination in QDSSC by the appropriate use of *molecular dipoles* and conformal coatings via *energy level alignment* (E. M. Barea, et al., 2010; M. Shalom, S. Ruhle, et al., 2009). Mesoporous TiO_2 electrodes were coated with "in situ" grown CdSe semiconductor nanocrystals by CBD. Surface modification of the CdSe sensitized electrodes by conformal ZnS coating and grafting of molecular dipoles (DT) has been explored to both increase the injection from QDs into the TiO_2 matrix and reduce the recombination of the QD sensitized electrodes. Different sequences of both treatments have been tested aiming at boosting the energy conversion efficiency of the devices. The obtained results showed that the most favorable sequence of the surface treatment (DT+ZnS) led to a dramatic 600% increase of photovoltaic performance compared to the reference electrode (without modification), and efficiency 1.60% under full 1 sun illumination was obtained (E. M. Barea, et al., 2010).

Ag_2S has an energy band gap of E_g~1.1eV (**Fig.1**), which is equal to the optimal band-gap of 1.13 eV for a PV cells (A. Marti & G. L. Araujo, 1996). Ag_2S QDs were synthesized using successive ionic layer adsorption and reaction (SILAR) deposition (A. Tubtimtae, et al., 2010). A 0.1 M $AgNO_3$ ethanol solution was prepared by dissolving $AgNO_3$ crystals in ethanol, then stirring vigorously for 30 min. A TiO_2 electrode was dipped into the 25°C $AgNO_3$ solution for 1 min, washed with ethanol, then dipped into a 0.1 M Na_2S methanol solution for 3 min. The two-step procedure forms one SILAR cycle, and was repeated several times. The assembled Ag_2S-QD solar cells yield a best power conversion efficiency of 1.70% and a short-circuit current of 1.54 mA/cm² under 10.8% sun. The solar cells have a maximal external quantum efficiency (EQE) of 50% at λ=530 nm and an average EQE about 42% over the spectral range of 400–1000 nm. The effective photovoltaic range covers the visible and near infrared spectral regions and is 2–4 times broader than that of the cadmium chalcogenide systems, the CdS and CdSe. The results show that Ag_2S QDs can be used as a highly efficient and broadband sensitizer for solar cells.

To increase the light absorption and raise the photoelectric conversion efficiency, porous oxide semiconductor is frequently used as one of the electrodes. One dimensional nanomaterials, such as nanotubes (D. R. Baker & P. V. Kamat, 2009; A. Kongkanand, et al., 2008), nanowires and nanorods (A. Belaidi, et al., 2008), and inversed opals (L. J. Diguna, et al., 2007a; K. Shankar, et al., 2009) are also excellent candidates (K. Shankar, et al., 2009; Y. Tak, et al., 2009). QD-SSC was designed and prepared by using CdS/CdSe co-sensitized TiO_2 nanotubes (TNT) on Ti wire and a highly active Cu_2S counter electrode (**Fig.4**). By optimizing the CdSe deposition time and length of nanotubes, a best efficiency of 3.18% was obtained under AM1.5 illumination (100mW cm^{-2}). It is revealed that there are several advantages of this fibrous QD-SSC based on TNT: (1) the conflict between illumination and opaque electrodes is effectively solved, in contrast to the situation based on Ti foil; (2) many more kinds of counter electrodes can be selected, giving the possibility of better photovoltaic performance and (3) it is flexible, of low serial resistance and easily weaved and integrated.

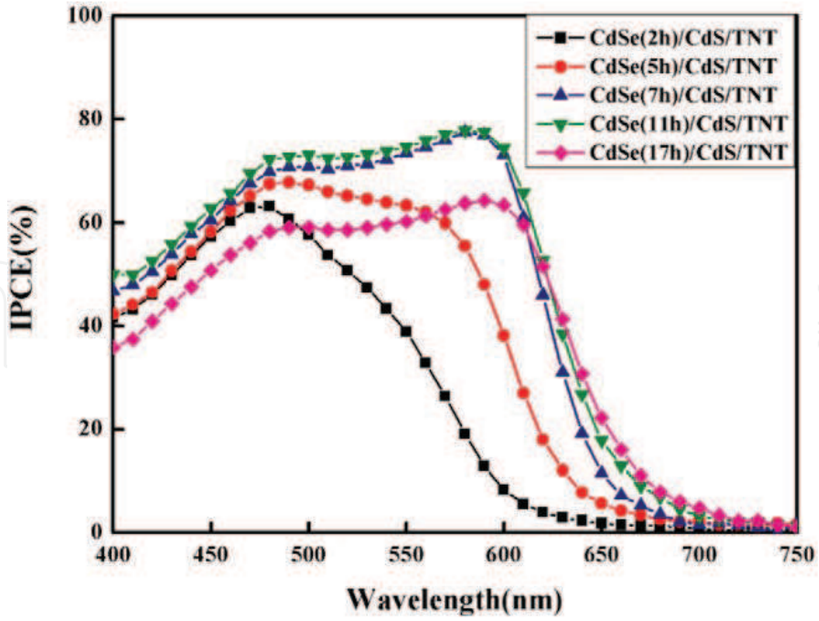

Fig. 4. Fibrous CdS/CdSe QDs co-sensitized solar cells based on ordered TiO_2 nanotube arrays.

Therefore, the fibrous QD-SSC is expected to have a potential application in the future (S. Q. Huang, et al., 2010).

In summary, nanocomposite QDSSCs work through two beneficial effects, (1) broaden spectral absorption range and (2) interaction between different absorbing parts reducing the overall recombination. QDSSCs have experienced rapid growth over the past two decades, and hold promising advantages over DSSCs. To achieve efficiency higher than the current record of 4.9%, the future directions in QDSSCs include (1) developing strategies to organize ordered assembles of two or more components (QDs and other semiconductors, metals, polymers) on electrode surfaces (J. Chen, et al., 2009), and gaining thorough understanding of the charge separation and transport (M. Shalom, S. Ruhle, et al., 2009); (2) developing new QDs that can harvest infrared photons to broaden the photo-response in the solar spectrum; (3) developing techniques to harvest hot (W. A. Tisdale, et al., 2010) or multiple charge carriers generated in QDs (A. J. Nozik, 2002); (4) synthesis and modification of various type of TiO_2, or other semiconductors, nanomaterials (X. B. Chen & S. S. Mao, 2006; Y. J. Lin, et al., 2009), and (5) modification of the physical properties of TiO_2 nanostructures to extend optical absorption into the visible region (X. B. Chen, et al., 2005; S. U. M. Khan, et al., 2002).

3.3 Polymer-inorganic PV cells

Polymer-based photovoltaic (PV) devices are of great interest, because they can be used to fabricate low-cost, light weight, large-area, and flexible solar cells using inexpensive painting or simple printing (Q. Q. Qiao, et al., 2008; M. K. Siddiki, et al., 2010). Hybrid polymer-based PV devices consisting of a conjugated polymer (p-type semiconductor) and inorganic semiconductors (n-type) have attracted attention as promising alternatives for future PV devices, since they combine the unique properties of inorganic semiconductors (e.g., high electron mobility and stability) with the good film-forming properties of conjugated polymers. Meanwhile, the size, shape, and optoelectronic properties of inorganic

semiconductor nanocrystals can be tailored during the synthesis process before the organic phase is incorporated. Conjugated polymers offer an attractive approach for increasing solar cell efficiencies because their band gaps and energy levels can be engineered by modifying their chemical structure (M. K. Siddiki, et al., 2010).

The highest theoretical energy conversion coefficiency for a single-junction polymer solar cell is about 10-13% for a polymer with a band gap of 1.5 eV (M. C. Scharber, et al., 2006). Multi-junction structures have appeared as a promising solution to achieve higher efficiency. Currently, a maximum 7.9% efficiency has been obtained (M. K. Siddiki, et al., 2010). New materials for broad spectrum light harvesting, highly efficient interfacial layer materials as both protection and recombination layer, and novel device designs are needed to increase the efficiency for large scale applications.

Tandem solar cells, in which two solar cells with different absorption characteristics are linked to use a wider range of the solar spectrum, has been fabricated with each layer processed from solution with the use of bulk heterojunction materials comprising semiconducting polymers and fullerene derivatives (J. Y. Kim, et al., 2007). A transparent titanium oxide (TiOx) layer separates and connects the front cell and the back cell. The TiOx layer serves as an electron transport and collecting layer for the first cell and as a stable foundation that enables the fabrication of the second cell to complete the tandem cell architecture. An inverted structure was used with the low band-gap polymer-fullerene composite as the charge-separating layer in the front cell and the high band-gap polymer composite as that in the back cell. Power-conversion efficiencies of more than 6% were achieved at illuminations of 200 mW/cm^2.

4. Solar hydrogen production via water splitting

In the various strategies for solar energy conversion, solar fuel or solar hydrogen conversion is attractive in that the harvested energy can be stored in chemical bonds. Since electricity only can be generated during day time by PV cells, large scale use of solar energy requires an efficient *energy storage* solution. Hydrogen is a "fuel of the future" because of its abundance and zero greenhouse gas emissions (S. Combs, 2008; G. W. Crabtree, et al., 2004). The splitting of water with sunlight to produce hydrogen is the basis for one of the most promising new energy industries, both in terms of high projected growth and low environmental footprint. Both water and sunlight are abundant resources, while hydrogen is a unique energy carrier since its oxidation leads to production of the starting material (water).

Once produced, hydrogen is the best transportation fuel, the most versatile, most efficient, most environmentally compatible, safest and most cost effective fuel to society (J. A. Turner, 1999; T. N. Veziroglu & F. Barbir, 1992). Prototypes of a number of hydrogen fuel cell devices are already on the market, including uses in cell phones, and even a self-sustained, hydrogen-operated house (D. Biello, 2008). The largest market segment is hydrogen use for transportation. Several cities, including Chicago and Vancouver, are already testing buses running on hydrogen in their public transit fleets, with plans to convert entire fleets to hydrogen. The hydrogen distribution infrastructure is also rapidly developing, with 74 hydrogen refueling stations already operational in the U.S. and Canada, and 43 more planned in the immediate future. The size of the current market ($1.5B) is limited to uses mandating the exploration of alternative energies. Efficient catalysts for solar hydrogen

production would make it possible to compete for the over $500B per year the US spends on oil.

Currently, most of the hydrogen is produced from methane-steam reforming (E. Kikuchi, et al., 2000), which consumes energy and produces green house gases emissions, mainly, carbon dioxide (W. Dougherty, et al., 2009). In contrast, the photoelectrochemical water-splitting process is a zero-emission process that only uses freely available solar energy (A. Currao, 2007). The problems of direct photochemical conversion of solar energy into hydrogen fall into the following categories: (1) inefficient use of solar spectrum for the generation of excitons (Wide bandgap semiconductors TiO_2, $SrTiO_3$, $KTaO_3$ that can split water directly use only UV wavelengths 4% of the total energy), (2) exciton recombination, and (3) inefficient use of dissociated electrons and holes in catalysis. Ever since the discovery of water-splitting by Fujishima and Honda in 1972 (A Fujishima & K. Honda, 1972), numerous studies have discussed these issues heavily to find a strong candidate material that overcomes these problems. The properties, size, geometry and compositions of materials are the keys to modify the material activity to improve hydrogen production (M. Ni, et al., 2007). Many tested semiconductors are either unstable in aqueous solution (CdS), or their band gap is too large to use light efficiently (SnO_2) (M. Matsuoka, et al., 2007). TiO_2 is chosen as the most stable semiconductor in water, but its large bandgap (3.2 eV) results in poor solar energy conversion. Currently, the use of visible light responsive quantum dots (including CdS, CdSe and PdSe) to improve the efficiency of TiO_2-based photovoltaics is an area of active exploration (T. Lopez-Luke, et al., 2008).

The advantage of photo-electro-chemical water splitting over water electrolyzing using solar PV cells. The current commercially available electrolyzers have electricity to hydrogen conversion efficiencies of up to 85%. To achieve a current density of about 1A/cm^2 that is normally used in electrolyzers, a cell voltage of 1.9V is required. Since the thermodynamic potential required for water splitting is 1.23eV, the energy conversion efficiency has an upper limit of 1.23/1.9=65% for the electrolyzers. Therefore, the PV-electrolyzer efficiency is limited to ~8% (O. Khaselev, et al., 2001; R. Van De Krol, et al., 2008). On the other hand, solar hydrogen production via direct photocatalytical reaction can be much higher, for example 16.8% for using a single semiconductor (A. B. Murphy, et al., 2006). Other advantages include the avoid of the significant fabrication and systems costs involved with the use of separate electrolyzers that are wired to p-n junction solar cells, and the easiness that an electric field can be created at a semiconductor-liquid junction (A. Heller, 1981).

Photoelectrochemical splitting of water involves the use of a semiconductor to convert solar energy into electrochemical energy and using it to split water. Advanced concepts in solar-fuel conversion share much in common with many third-generation concepts for solar cells. Suitable photo-electrode materials for efficient solar hydrogen generation have to fulfill the following requirement: (1) strong (visible) light absorption, (2) high chemical stability, (3) suitable band edge positions to enable reduction/oxidation of water, (4) efficient charge transport in the semiconductor, (5) low overpotential for the reduction/oxidation reaction, and (6) low cost (R. Van De Krol, et al., 2008).

The first requirement is related to solar spectrum and energy requirement for chemical reaction. The minimum band gap of the semiconductor for photo water splitting is determined by the energy required to split water (1.23 eV), plus the thermodynamic loss (~0.4eV) (M. F. Weber & M. J. Dignam, 1986), and the over-potentials that are required to

ensure sufficient fast reaction kinetics (~0.3-0.4eV) (J. R. Bolton, et al., 1985; A. B. Murphy, et al., 2006). So, the low limit of band gap is 1.9 eV, which corresponding to light wavelength of 650 nm, in the lower energy red portion of the visible spectra. Since the sunlight intensity drops rapidly below 400 nm (corresponding to 3.1 eV), the suitable band gap for the semiconductors is 1.9~3.1eV, which is in the visible range of the solar spectrum. Murphy *et al.* predicted a maximum efficiency of 16.8% for a hypothetically idea material with a band gap of 2.03eV (A. B. Murphy, et al., 2006), which exceeds the 10% target by 2018 set the U.S. Department of Energy for photoelectrochemical hydrogen production (Us_Department_of_Energy, 2007). Higher efficiencies can be obtained using a multiple band gap system. *Nanocomposites are needed to construct a system to meet the requirement of visible-light absorption.*

The second requirement excludes non-protected direct use of most non-oxide semiconductors, such as Si, GaAs, GaP, CdS, which either dissolve or form a thin oxide film that prevent electron transfer across the semiconductor-electrolyte interface. For thermodynamic stability, a semiconductor's reductive and oxidative decomposition potentials must be more negative than the semiconductor's conduction band-edge for water reduction or more positive than the semiconductor valence band-edge potential for water oxidation, respectively (O. Khaselev & J. A. Turner, 1998b). Photo generated holes are able to oxide most metal oxides, but photo-corrosion can be avoided if the charge transfer across the interface to oxidize water is faster than the decomposition reaction. TiO_2 and SnO_2 show excellent stability over a wide range of pH values and applied potential, while ZnO always decomposes and the stability of Fe_2O_3 depends on the present of dopants, pH, and oxygen stoichiometry (R. Shinar & J. H. Kennedy, 1982). Generally speaking, wide bandgap metal oxides semiconductors are stable against photo-corrosion and small band gap semiconductors are not, in contradiction to the first requirement. This is the so called "duality principle" limitation of photoelectrolysis (N. S. Lewis, 2001). Therefore, *nanocomposites are needed to solve the photo-corrosion problem*.

Fig.1 shows the band-edge positions of various semiconductors. For photo water splitting, the conduction and valence band edges should straddle the reduction and oxidation potential of water: the conduction edge should above $E_{red}(H^+/H_2)$ and the valence edge should below $E_{ox}(OH^-/O_2)$. Most non-oxide semiconductors are able to reduce, but not oxidize water; and most oxide semiconductors are able to oxidize, but not reduce water. After photo-excitation and charge separation in an n-type semiconductor, holes in the VB diffuse to the semiconductor-liquid interface to oxidize water. The large difference between the VB of oxide semiconductors (~3eV vs NHE, *cf.* Fig.1) and the oxygen evolution reaction (OER) potential (1.23 eV vs NHE) indicate, much of the excess energy (~1.77eV) is wasted by thermal relaxation. Therefore, the efficiencies converting sunlight to O_2 of most photoanodes are very low.

Wide band gap metal oxide semiconductors absorb only a small portion of the solar spectrum (UV part). By using a tandem cell approach, the remaining part of the spectrum can be used to provide the additional bias voltage required for the reduction reaction. For example, a *separated* DSSC was used to provide a bias voltage to WO_3 or Fe_2O_3 photo-anode (involving two separated devices). An efficiency of 4.5% was achieved for WO_3 photo-anode (M. Gratzel, 2001), which is close to the theoretical efficiency WO_3 (A. B. Murphy, et al., 2006). Using highly efficient dendritic α–Fe_2O_3 photo-anodes, overall solar-to-hydrogen efficient 2.2% are reached (A. Kay, et al., 2006). A *monolithic* tandem cell (involving only a

single-device) based on a p-type $CaInP_2$ photo-cathode biased by a GaAs p-n junction solar cell was fabricated, and the solar-to-chemical conversion efficiency is 12.4% (O. Khaselev & J. A. Turner, 1998a). The shortcomings of this device are *high* ***cost*** and severe photo-corrosion problem. Amorphous silicon (a-Si) is much cheaper than GaAs-based materials. The a-Si/WO_3 hybrid photo-electrodes show solar-to-hydrogen conversion efficiencies of 1% in out-door test (E. L. Miller, et al., 2005). A particular challenge for such device fabrication is to deposit the metal oxides at sufficiently low temperatures (<300^{o}C) to avoid degradation of the underlying a-Si junctions.

In the *composite particle systems*, a hetero-junction forms between two component-particles. Due to the different energetic positions of the conduction and valences edges, the electrons are transported to one component-particle, while the holes move to the other one. The effective charge separation in such systems limits the recombination of photo-excitons; hence improve the sun-to-hydrogen conversion efficiency. In the *mixed-particle systems*, this concept is taken a step further by perform the oxidation and reduction of water on two different particles that are not in direct contact. To ensure a complete redox reaction at each individual particle, a redox mediator, for example I^-/IO_3 (K. Sayama, et al., 2001), is used to transport electrons from the oxygen evolving particles to their hydrogen evolving counterparts.

Even though several semiconductors have band-edge positions that are appropriate for water reduction or oxidation, the kinetics of these reactions on the bare semiconductor surface generally limit the efficiency. Addition of a ***co-catalyst*** to the surface can improve the reaction kinetics. Pt is the frequently used co-catalyst for hydrogen evolution reaction (HER). Nobel metals and transition metals, such as Au, Ag, Cu and Ni, can be also effective and cheaper (N. Alenzi, et al., 2010; M. G. Walter, et al., 2010). On the other hand RuO_2, IrO_2 can be effective co-catalysts for OER (M. G. Walter, et al., 2010). When the noble metals are loaded to the surface of a semiconductor, they act as electron traps because their lower Fermi energy level than the semiconductor, facilitating electron-hole separation and promotes interfacial electron transfer process (V. Subramanian, et al., 2001). In addition, surface plasmon resonances of noble metal particles, which can be excited by visible light, increase the electric field around metal particles and thus enhance the surface electron excitation and electron-hole separation on noble metal-doped semiconductor particles (Y. M. Cho & W. Y. Choi, 2002; E. Kowalska, et al., 2010). The role played by the co-catalyst is extremely important. It improves overall photocatalytical activity of the water splitting. In many cases, the photo-catalyst is only able to evolve either hydrogen or oxygen gas, not both at the same time. If only hydrogen (oxygen) evolves, a sacrificial electron donor (accepter) must be present to ensure the stoichiometric consumption of electrons and holes. The sacrificial systems are of considerable interest because they permit the study of electrode reactions. Methanol is almost always used as a sacrificial electron donor (hole scavenger) (E. L. Miller, et al., 2005).

4.1 CdS

CdS is a fascinating visible light-driven photocatalyst for water splitting having a band-gap energy of 2.4 eV. Its CB and VB positions are very suitable for HER and OER, respectively. However, CdS is very unstable toward photocorrosion due to serious self oxidation of the photogenerated holes in the valence band ($2h^+_{vb}+CdS \rightarrow Cd^{2+}+S$). CdS nanocrystals, nanowires, and nanorods were synthesized and used to study photo

hydrogen production using sacrificial reagents under visible light irradiation (N. Bao, et al., 2007; J. S. Jang, et al., 2007; Y. Li, et al., 2009). A high quantum yield of about 60% measured(N. Z. Bao, et al., 2008) at 420 nm was obtained for hydrogen production over nanoporous CdS nanostructures attributed the high efficiency to the efficient charge separation, fast transport of the photo-generated carriers, and fast photochemical reaction at the CdS/electrolyte interface.

Among the CdS composites, CdS-TiO_2 has attracted the most extensive research (X. B. Chen, et al., 2010; T. Y. Peng, et al., 2008). Both the conduction and valence band edges of CdS are at more negative potentials than those of TiO_2 (*cf.* Fig.1). Under visible-light irradiation, the photogenerated electrons in the CdS particles quickly transfer to TiO_2 particles, whereas photogenerated holes stay in CdS. This facilitates the electron-hole separation and prevents the charge recombination, improving the photocatalytical activity.

CdS-Au-TiO_2 heterojunction was developed where CdS, TiO_2 and the electro-transfer medium Au were all spatially fixed. This three-component system exhibits a high photocatalytical activity, far exceeding those of the single- and two-component systems, as a result of vectorial electron transfer driven by the excitation of both TiO_2 and CdS (H. Tada, et al., 2006). General speaking, a ***Z-scheme*** water splitting involve two step photo-excitation under visible light irradiation mimicking the nature photosynthesis of green plants (K. Sayama, et al., 2002). The Z-scheme system consisted of a H_2-evolution photocatalyst (PS1), an O_2-evolution photocatalyst (PS2), and a reversible redox mediator (Ox/Red) which acts separately as electro donor (PS1) and acceptor (PS2) for the respective half reaction and which is different from irreversible sacrificial reagents used in conventional systems. CdS-Au-TiO_2 is an all-solid-state Z scheme (PS1:CdS, PS2:TiO_2 and Au is the electro-transfer system). The electron supply from TiO_2 to CdS via Au restricts the self-decomposition of CdS due to the oxidation of surface S^{2-} ions by the photogenerated holes in CdS. In a Z-scheme system, H_2 and O_2 are evolved separately from two different photocatalysts, which restrains the back-reaction of water decomposition to some extent.

In the CdS, TiO_2 and Pt system (H. Park, et al., 2008), the direct particle to particle contact of CdS and TiO_2, and the photodeposition of Pt on the TiO_2 particle surface which resulted in the vectorial electron transfer of CdS →TiO_2 →Pt were necessary to achieve efficient charge separation and transfer, hence the observed highest photoactivity of the CdS/(Pt-TiO_2) hybrid catalyst. The photocatalytic activity of CdS could be enhanced significantly by loading a small amount of a noble metal sulfide (PdS, Rh_2S_3, Ru_2S_3), as well as a noble metal (Pt, Pd, Ru, Rh) (H. J. Yan, et al., 2009). Moreover, co-deposition of Pt with other noble metal sulfides on CdS demonstrated further enhanced photoactivity in hydrogen production; the photocatalytical activity of CdS co-deposited with Pt and PdS was greater than those of Pt/CdS and PdS/CdS. This synergistic effect between the Pt and PdS cocatalysts could be explained by the fact that the two cocatalysts may facilitate separation of the photogenerated electrons and holes on the photocatalyst.

Nanostructured Ag_2S/CdS were synthesized by a two-step precipitation method with Ag_2S (*cf.* Fig.1) (S. H. Shen, et al., 2010), the photoactivity was evaluated by hydrogen evolution from aqueous solution containing Na_2S/Na_2SO_3 as a hole scavenger under simulated solar light (AM1.5). When the concentration of Ag_2S was 5% by weight, Ag_2S/CdS showed the highest photocatalytical activity for hydrogen evolution due to the efficient electron-hole separation, with the solar-hydrogen energy conversion efficiency approximately 0.7%.

The transition-metal sulfides have also been developed as novel cocatalysts. The CdS activity was enormously increased by loading with MoS_2, even higher than that of Pt-loaded CdS under the same reaction conditions (X. Zong, et al., 2010). The better coupling between the structures and electronic configurations of MoS_2 and CdS together, and the formation of junctions between CdS and MoS_2, improved the charge separation and were mainly responsible for the high activity of this MoS_2/CdS catalyst. The MoS2 activated the photocatalyst by reducing the electrochemical proton reduction overpotential (F. A. Frame & F. E. Osterloh, 2010).

CdSe and CdS have been used to co-sensitize nitrogen doped TiO_2 (N:TiO_2) (J. Hensel, M. Canin, et al., 2010). The CdSe/CdS/N:TiO_2 electrodes has much higher photoelectrochemical (PEC) response as well as incident photon to charge efficiency (IPCE) than the CdSe/CdS/TiO_2 electrodes. This was attributed to increased hole transport from CdS to oxygen vacancy levels introduced into the TiO_2 upon nitrogen doping. This increased hole transport reduces undesired electron hole recombination in the CdS layer that otherwise tends to reduce PEC performance. The results demonstrate the importance of engineering the band structure of metal oxide nanocomposite structures for PEC and other applications.

In a heterostructure where a CdSe seed encapsulated in a CdS rod which is tipped with a Pt particle (**Fig.5**) (L. Amirav & A. P. Alivisatos, 2010), the holes were three-dimensionally confined to the CdSe seed while the delocalized electrons were transferred to the metal tip, so the electrons were separated from the holes over three different components and by the tunable physical length of the CdS rod. By tuning the nanorod heterostructure length and the size of the seed, the hydrogen production acitivity was significantly increased compared to that of the unseeded rods. This structure was highly active for hydrogen production with an apparent quantum yield of **20**% at 450 nm wave length. There was also a demonstrated improved stability compare to CdS rods without CdSe seeding. Among all the systems studied involving CdS so far, this heterostructure yielded the *highest* hydrogen production activity, 40,000 μmol/h/g (X. B. Chen, et al., 2010).

To improve their photocatalytical stability and photoactivity, sulfides, such as CdS, have been intercalated into the layers of some layered metal oxide. The photocatalytical activities for hydrogen evolution of CdS-intercalated composites were superior to those of CdS alone or to a physical mixture of CdS and the metal oxides (W. F. Shangguan, 2007). The improvement was attributed to the quick transfer of the photogenerated electrons from CdS to the metal oxides through the layered nanostructure.

4.2 AgCl/AgBr

Thin silver chloride (AgCl) layers evolve oxygen under UV/vis illumination in aqueous solution under appropriate conditions. AgCl deposited on a conducting support photocatalyzes the oxidation of water to O_2 in the presence of a small excess of silver ions in solution. The light sensitivity in the visible part of the spectrum is due to self-sensitization caused by reduced silver clusters which has CB significantly positive that that of AgCl (D. Schurch, et al., 2002). Considerable improvement of sensitivity has been observed with AgBr sensitized AgCl photoanodes. Similar to CdS and CdSe, the bandgap edges of AgBr straddle the HER and OER potentials (*cf.* **Fig.1**). The AgCl photoanode was combined with hydrogen-producing semiconductors, a platinized silicon solar cell or platinized p-$GaInP_2$ to reduce water to hydrogen. Direct water splitting use AgBr only has not been performed yet.

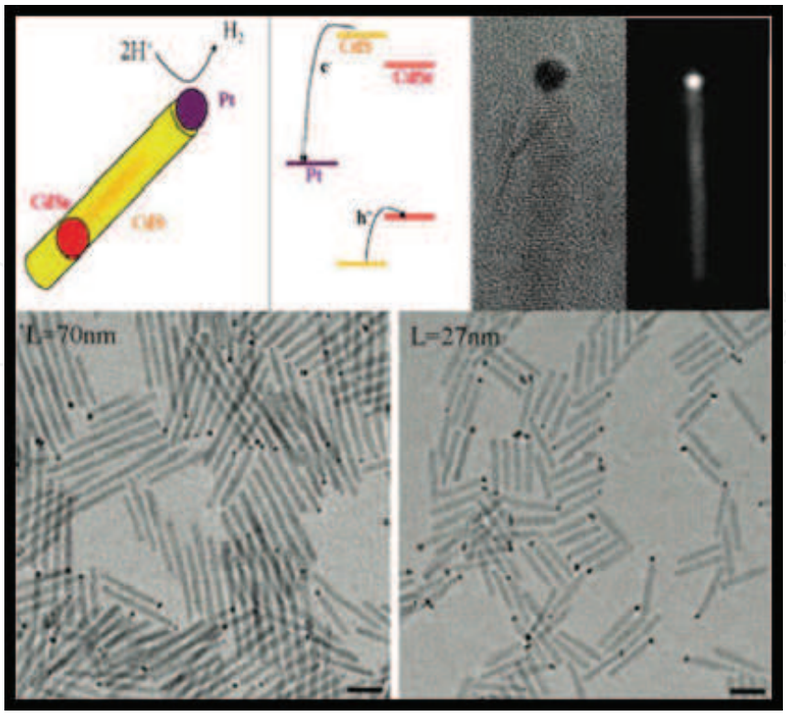

Fig. 5. Heterostructure of CdSe-CdS-Pt.

4.3 $InVO_4$

$InVO_4$ has band gap of about 2.0 eV (**Fig.1**) and was found to be a new visible light responding photocatalyst for water decomposition (J. H. Ye, et al., 2002). The photocatalyst showed activity to visible light in a wide wavelength range up to 600 nm. The photocatalytical water splitting activity increases significantly by loading NiO as a co-catalyst. The evolution rate of H_2 from water has achieved about 5 μmol/(g·h) under visible light (λ>420nm) of a 300W Xe arc lamp.

The mesoporous photocatalyst $InVO_4$ was synthesized by the template-directing self-assembling method (L. X. Xu, et al., 2006). The crystal structure of $InVO_4$ could be controlled by changing the calcination temperature. Compared with the anatase TiO_2 and conventional $InVO_4$, the mesoporous $InVO_4$ was more responsive toward visible light. The evolution rate of H_2 from water over the mesoporous $InVO_4$ achieved 1836 μmol/(g·h) under UV light irradiation, which was much higher than the anatase TiO_2 and conventional $InVO_4$.

4.4 CdSe

Nanocomposite materials based on visible-light-absorbing CdSe QDs and N-doped TiO_2 nanoparticles and nanowire arrays with properties tailored for PEC hydrogen generation. The experiments demonstrated that the synergistic effect of sensitization *and* elemental doping significantly enhances the photoelectrochemical activities of the TiO_2 nanostructured photoanodes (**Fig.6**) (J. Hensel, G. M. Wang, et al., 2010). These composite nanostructures show enhanced overall charge transport and improved PEC performance when the relevant band gap states are properly aligned and utilized. Enhanced electron-hole separation and hole transfer/transport through the oxygen vacancy states, Vo, mediated by N-doping has

been proposed to explain the observed experimental results. Such nanocomposite structures simultaneously enhance visible light absorption and interfacial charge transfer. The results provide useful insights for developing new nanostructures tailored for PEC hydrogen generation and other applications via controlled band engineering.

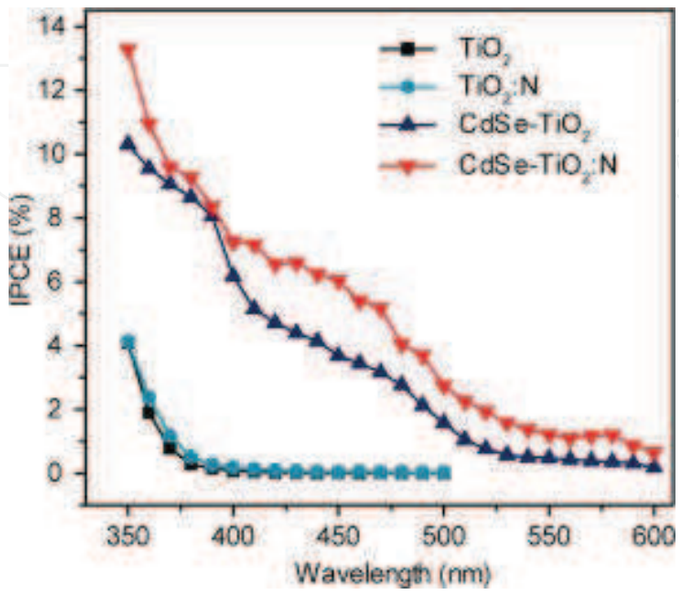

Fig. 6. Synergy of CdSe QDs sensitization and N-doping of TiO_2.

Under visible light irradiation, CdSe-nanoribbons photocatalyze H_2 evolution from aqueous sodium sulfite/sulfide solution with a quantum efficiency of 9.2% at 440 nm, whereas bulk CdSe is not active for the reaction. Photoelectrochemical measurements show that the activity of nano-CdSe is caused by a raised flatband potential (-0.55 V, NHE) which follows from the increased bandgap (2.7 eV) of this quantum confined material. In the presence of a sulfide ion, the flatband potential is fixed to -0.43 V (NHE), slightly below the sulfide redox potential (-0.48 V, NHE). When the nanoribbons are chemically linked to MoS_2 nanoplates that were obtained by exfoliation and ultrasonication of bulk MoS_2, the activity increases almost four times, depending on the mass percentage of MoS_2. Cyclic voltammetry reveals that the enhancement from the MoS_2 nanoplates is due to a reduction of the H_2 evolution overpotential (F. A. Frame & F. E. Osterloh, 2010). In contrast, chemical linkage of Pt nanoparticles to the nanoribbons does not affect the photocatalytical activity.

4.5 Eosin Y sensitized CuO-TiO_2

It has been demonstrated that the dye-sensitized CuO/TiO_2 can be used as photocatalyst for hydrogen production from Diethanolamine–H_2O mixture with high quantum efficiencies under visible light irradiation ($\lambda > 420$ nm). Eosin Y sensitized CuO/TiO_2 photocatalysts were very active and stable for hydrogen generation. The addition of CuO strongly improved the adsorption capability of TiO_2 toward eosin dye. The electrons excited from the sensitizer molecules by the visible light injected into the conduction band (CB) of both TiO_2 and CuO, the electrons in CB of TiO_2 subsequently transferred to CB of CuO, which resulted in a build-up of excess electrons in the conduction band of CuO. Consequently, the accumulation of excess electrons in CuO causes a negative shift in the Fermi level of CuO

which gains the required overvoltage necessary for sufficient water reduction reaction. As a result, the significant enhancement of apparent quantum yield and a good stability was obtained over the dye-sensitized 1.0 wt% CuO/TiO_2 photocatalyst. The function of CuO is to help the charge separation and to act as a water reduction size. In the presence of triethanolamine, acetonitrile and triethylamine, the photocatalyst can catalyze hydrogen evolution over 120 h. The highest quantum efficiency obtained was about 5.1%.

4.6 MoS_2

Molybdenum disulfide (MoS_2) is a layered semiconductor that exhibits both quantum confinement and excellent catalytic activity for HER when nanostructured (J. Bonde, et al., 2008; T. F. Jaramillo, et al., 2007). In the bulk, its conduction band sits below the HER potential (J. P. Wilcoxon & G. A. Samara, 1995) and its band gap of 1.2 eV is too small to drive water splitting without a bias. Nanostructured MoS_2 could potentially alleviate these limitations while further improving charge transport by minimizing the distance of travel for photogenerated charge carriers. In addition, MoS_2 is a material that has previously exhibited excellent photocatalytical stability (H. Tributsch & J. C. Bennett, 1977) and is a highly scalable, widely used industrial catalyst (R. R. Chianelli, et al., 2006) and solid lubricant (C. Muratore & A. A. Voevodin, 2009).

MoS_2 nanostructures were synthesized and their electrochemical activity was investigated for hydrogen evolution and photoelectrochemical water splitting (Z. B. Chen, et al., 2010). MoS_2 nanoparticles were made using a reverse micelle encapsulation method and exhibit quantum confinement of the indirect band gap up to 1.8 eV. A MoS_2 double-gyroid bi-continuous structure was made using an evaporation induced self assembly method. Both nanostructures exhibit improved activity for the hydrogen evolution reaction versus bulk MoS_2. Photoelectrochemical activity was also observed in both nanostructures (Z. B. Chen, et al., 2010).

UV-light irradiation to TiO_2 in an aqueous ethanol solution of $(NH_4)_2MoS_4$ under deaerated conditions has yielded molybdenum (IV) sulfide nanoparticles on a TiO_2 surface (MoS_2/TiO_2). In HCOOH aqueous solutions, the MoS_2/TiO_2 system exhibits a high level of photocatalytical activity for H_2 generation (S. Kanda, et al., 2011).

4.7 WO_3

WO_3 has been suggested as a candidate material for PEC hydrogen production as earlier as 1976 (G. Hodes, et al., 1976). It can be fabricated using low-cost processes, such as anodic oxidation, chemical vapor deposition, sol-gel as well as reactive sputtering (N. Gaillard, et al., 2010). In the case of integration over low-cost amorphous silicon-based solar cells to form hybrid-photo-electrode (HPE) device, reactive sputtering is of great interest because of its low deposition temperature capabilities (from 200°C to 300°C). From an electrochemical point of view, tungsten oxide corrosion resistance in acidic solutions has been already demonstrated (M. A. Petit & V. Plichon, 1996) and its excellent behavior as a device under various PEC operations has been widely reported (C. G. Granqvist, 2000; C. Santato, et al., 2001). Due to its wide band gap (2.6eV), tungsten oxide framework or optoelectronic properties modification using foreign element incorporation such as silicon, molybdenum or nitrogen became of great interest. However, no modified tungsten oxide-based thin film material has yet surpassed pure WO_3 PEC performances, with a saturation photocurrent density of approximately 3.0 $mAcm^{-2}$ in acidic solution under AM1.5G illumination (R.

Solarska, et al., 2010), which is only 50% of the theoretical value based on pure WO_3 bandgap (6% STH efficiency) (Z. B. Chen, et al., 2010), assuming a complete collection and conversion to electronic current of photogenerated electron hole pairs. Thus, improvement of tungsten oxide-based PEC devices performances is theoretically possible.

Polycrystalline WO_3 thin films for photoelectrochemical hydrogen production were investigated using photoelectron spectroscopy and inverse photoemission. A careful study has minimized X-ray and electron beam-induced degradation and combined ultraviolet photoelectron spectroscopy and inverse photoemission determined the surface positions of the valence and conduction band edges, respectively, and the work function (i.e., the position of the vacuum level). This allows to paint a completely experiment-based picture of the WO_3 surface level positions, which are of central relevance for the photoelectrochemical activity of such surfaces (L. Weinhardt, et al., 2008). It was found that the WO_3 surface to be wide gap (3.28±0.14) eV and n-type, with the conduction band minimum 0.39±0.10 eV above the Fermi level and 0.31±0.11 eV above the H^+/H_2 reduction potential. The valence band maximum is 2.89±0.10 eV below the Fermi level and 1.74±0.11 eV below the H_2O/O_2 oxidation potential (L. Weinhardt, et al., 2008).

In both PV and PEC cells, improved performance and higher conversion efficiency can be obtained using diode structures combining suitable n-type photoanodes and p-type photocathodes which lead to efficient electron-hole separation (M. Gratzel, 2001; O. Khaselev & J. A. Turner, 1998a; A. J. Nozik, 1976). A p-Cu_2O (band gap 2.0eV)/n-WO_3 (band gap 2.6eV) coupling system was developed to avoid back reaction of the photo-induced charges (C. C. Hu, et al., 2008), and resulted in higher photocatalytical hydrogen production.

Mo incorporation in the entire WO_3 film (WO_3-Mo) results in poor PEC performances, most likely due to defects that trap photo generated charge earners. However, compared to a pure WO_3, a 20% increase of the photocurrent density at 16 V vs SCE is observed for WO_3-Mo based PEC electrode if the Mo incorporation is limited to the near-surface region of the WO_3 film. The resulting WO_3/WO_3-Mo bilayer structure is formed by epitaxial growth of the WO_3-Mo top layer on the WO_3 bottom layer, which allows an optimization of the electronic structure induced by Mo incorporation while maintaining good crystallographic properties (N. Gaillard, et al., 2009). The WO_3-Mo films were found in a recent study (M. Bar, et al., 2010) to be n-type with an electronic surface band gap of 3.27±0.15 eV. The conduction band minimum (valence band maximum) is 0.64±0.10 eV above (2.63±0.10 eV below) the Fermi level and at most 0.38±0.11 eV above the H^+/H_2 reduction potential (at least 1.66±0.11 eV below the H_2O/O_2 oxidation potential). The conduction band of WO_3:Mo is shifted upwards (further away from the reduction potential compared to WO_3) while maintaining a valence band position which is still sufficiently low with respect to the oxidation potential) for PEC operation. The findings suggest an explanation why WO_3:Mo/WO_3 bilayer structures show improved photoelectrochemical performance compared to respective single layer photoanodes (M. Bar, et al., 2010). The bilayer approach, i.e., the deliberate decoupling of the tailored electrode surface from its bulk properties may open a new promising route for the development of next-generation PEC materials.

A new device integration scheme was presented recently to increase photocurrent density using highly textured substrates (HTS) (N. Gaillard, et al., 2010), which were obtained by anisotropic etching of [100] silicon substrates in KOH solution. A very good coverage of WO_3 onto the silicon pyramids and a photocurrent doubling is observed when compared to WO_3 deposited on flat silicon substrates.

4.8 F_2O_3

Early studies identified haematite (α-Fe_2O_3) as potential photoanode material for water splitting (J. H. Kennedy & K. W. Frese, 1977; J. H. Kennedy & M. Anderman, 1983; R. K. Quinn, et al., 1976). Recent work has focused on developing films that could be used as part of tandem photoelectrolysis cells, in which high energy photons are used to drive the oxidation of water by photogenerated holes at the Fe_2O_3 surface, and lower energy photons transmitted through the oxide are harvested by a solar cell that applies a bias voltage to the photoelectrolysis cell. Recent optimization of the morphology and doping of nano-structured thin films of Fe_2O_3 have resulted in substantial improvements in the photocurrent response (I. Cesar, et al., 2009; S. Saremi-Yarahmadi, K. G. U. Wijayantha, et al., 2009; S. Saremi-Yarahmadi, A. A. Tahir, et al., 2009).

Photoelectrochemical Impedance Spectroscopy (PEIS) has been used to characterize the kinetics of electron transfer and recombination taking place during oxygen evolution at illuminated polycrystalline α-Fe_2O_3 electrodes prepared by aerosol-assisted chemical vapor deposition from a ferrocene precursor (K. G. U. Wijayantha, et al., 2011). The complex potential dependence of the rate constants for these two processes highlights the non-ideal nature of the α-Fe_2O_3–electrolyte interface arising from photogenerated surface species. Efficient water splitting in a tandem photoelectrochemical cell using α-Fe_2O_3 as a photoanode requires that the photocurrent onset should be as close to the flatband potential as possible, about 0.8 V negative of the reversible oxygen electrode potential. A positive displacement of the photocurrent onset represents a loss of free energy and hence of efficiency. Clearly this means that accumulation of positive surface charge associated with Fermi level pinning and changes in surface composition must be avoided as far as possible. Since the accumulation of electronic and ionic surface charge appears to be associated with sluggish hole transfer kinetics, it should be possible to overcome the effects by using a suitable surface catalyst for the oxygen evolution reaction. The PEIS analysis also shows that the limiting factor determining the performance of the α-Fe_2O_3 photoanode is electron–hole recombination in the bulk of the oxide. The minimization of the loss of holes can be achieved at least in part by growing nano-structured thin films in such a way that the dimensions are comparable with the width of the space charge region (J. Brillet, et al., 2010; F. Le Formal, et al., 2010). Other promising approaches include using oriented nanorod arrays (R. Van De Krol, et al., 2008), or a host–guest structure in which small α-Fe_2O_3 particles are deposited on a porous oxide substrate such as WO_3 (K. Sivula, et al., 2009).

To improve the optoelectronic properties of iron oxide as a photoelectrode, hematite (α-Fe_2O_3) thin films were doped with titanium using atmospheric pressure chemical vapor deposition (APCVD) for synthesis (P. Zhang, et al., 2011). The films were prepared by pyrolysis of $Fe(CO)_5$ and $TiCl_4$ precursors on fluorine-doped tin oxide (FTO) substrates and found to have a polycrystalline morphology with faceted particulates about 20 to 50 nm in size with a preferred crystallographic growth along the [110] direction (direct band gap with a value of ~2.1 eV). The performance of the photoanodes was measured as a function of titanium concentration. A maximum efficiency was observed at about 0.8 atom% Ti in hematite. The Incident Photon-to-current Conversion Efficiency (IPCE) to hydrogen was measured in alkaline electrolyte. Under an applied bias of 0.6 V vs. Ag/AgCl at 400 nm the IPCE for water splitting in alkaline solution was found to be 27.2%, the highest efficiency reported for Ti doped hematite photoanodes. The IPCE of the Ti doped hematite sample at the lower bias (6% at 0.4 V vs. Ag/AgCl) is relatively low which is associated with a large

photocurrent onset potential (0.2V), which suggested a high density of trap states located below the conduction band edge.

An experimental study of the influence of gold nanoparticles on an α-Fe2O3 photoanodes for photoelectrochemical water splitting is described (E. Thimsen, et al., 2011). A relative enhancement in the water splitting efficiency at photon frequencies corresponding to the ***plasmon resonance*** in gold was observed. This relative enhancement was observed only for electrode geometries with metal particles that were localized at the semiconductor-electrolyte interface consistent with the observation that minority carrier transport to the electrolyte is the most significant impediment to achieving high efficiencies in this system.

4.9 Ternary oxides

The oxides are privileged materials for the water photo-splitting owing to their chemical inertness in aqueous electrolytes. For oxides without partially filled d-levels, an empirical relationship was found between the flat band potential (V_{cb}) and energy gap E_g: $V_{cb,VNHE}$ =2.94-E_g (D. E. Scaife, 1980). Oxides having an optical gap around 1.4 eV are particularly interesting for the terrestrial applications but most of them have either unsuitable potential V_{cb} for hydrogen evolution reaction. Rewriting the equation, E_g=2.94- $V_{cb,VNHE}$, we see that for suitable $V_{cb,VNHE}$ (~-0.5 eV), the band gaps will be very wide (>3 eV). They absorb only in the UV region because of their large forbidden band (Eg) and the quantum yields are generally low.

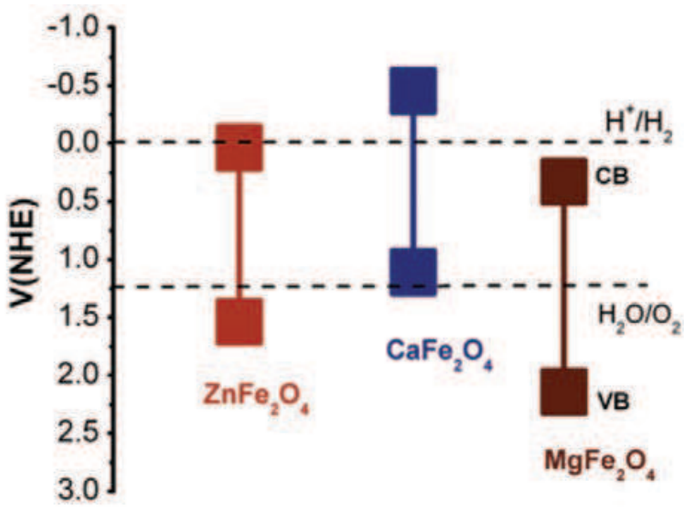

Fig. 7. Band gaps of spinels.

Ternary oxides $CuMO_2$ crystallizing in the delafossite structure begins to receive interest in the field of the photoelectrochemistry owing to their interesting properties of band gap modulation and pH-insensitivity of the electronic bands (A. Derbal, et al., 2008). The delafossite $CuFeO_2$ has been prepared by thermal decomposition from various salts. The polarity of generated voltage is positive indicating that the materials exhibit p-type conductivity whereas the electroneutrality is achieved by oxygen insertion. $CuFeO_2$ is a narrow band gap semiconductor with an optical gap of 1.32 eV. The oxide was characterized photoelectrochemically; its conduction band (-1.09 V-RHE) is located below that of SnO_2 (-0.86 V-RHE) at pH 13.5, more negative than the H_2O/H_2 level leading to a

thermodynamically favorable H_2 evolution under visible irradiation. The sensitizer $CuFeO_2$, working as an electron pump, is stable towards photocorrosion by hole consumption reactions involving the reducing agents X^{2-} (i.e., $S_2O_3^{2-}$ and SO_3^{2-}). The photoactivity was dependent the precursor and the best performance (1160 μmol/hg) was obtained in $S_2O_3^{2-}$ (pH 13.5) over $CuFeO_2$ synthesized from nitrate with a mass ratio ($CuFeO_2/SnO_2$) equal to unity. A quantum yield of 0.5% was obtained under polychromatic light (A. Derbal, et al., 2008).

The physical properties and photoelectrochemical characterization of the spinel $ZnFe_2O_4$ have been investigated for the hydrogen production under visible light (S. Boumaza, et al., 2010). The forbidden band was found to be 1.92 eV and the transition is indirectly allowed. The electrical conduction occurs by small polaron hopping with activation energy of 0.20 eV. *p*-type conductivity is evidenced from positive thermopower and cathodic photocurrent. The flat band potential (-0.33 VNHE) determined from the capacitance measurements is suitably positioned with respect to H^+/H_2 level. Hence, $ZnFe_2O_4$ was found to be an efficient photocatalyst for hydrogen generation under visible light. The photoactivity increases significantly when the spinel is combined with a wide band gap semiconductor. The best performance with a hydrogen rate evolution of 410,688 μmol/hg concurs over the hetero-system $ZnFe_2O_4/SrTiO_3$ in $Na_2S_2O_3$ (0.025 M) solution, which is the *record high* among all the photocatalysts studied so far (X. B. Chen, et al., 2010).

Nanocrystalline photocatalysts of spinel $MgFe_2O_4$, $ZnFe_2O_4$ and orthorhombic $CaFe_2O_4$ oxides were synthesized (at low temperature about 973 K) by microwave sintering, in one sixtieth of the time required to that of the conventional method (R. Dom, et al., 2011). A significantly improved crystallinity was obtained for the samples irradiated for longer duration of time (10-100 min). The theoretically computed electronic structure of the MFe_2O_4 (M: Ca, Zn, Mg) systems was respectively correlated with the experimental results obtained from their structural and photocatalytical characterization. The photocatalytical performance was found to be affected by surface area and crystallinity of the photocatalyst. The density functional theory (DFT) calculations of MFe_2O_4 lattices revealed that M-ion controllably affects the density of sates of the Fe-*d* orbitals near the Fermi level. Consequently they play an important role in determining the band-energetics and thus the visible light photocatalytical activity for methylene blue degradation (**Fig.7**).

4.10 Water splitting systems

Over the past several decades, a number of photocatalysts have been successfully developed to construct an overall water-splitting system for simultaneous hydrogen and oxygen generation in the absence of sacrificial reagents (Z. G. Zou, et al., 2001), Among which $(Ga_{1-x}Zn_x)(N_{1-x}O_x)$ has been proven as the most promising (X. B. Chen, et al., 2010; K. Maeda, et al., 2008). Steady and stoichiometric H_2 and O_2 evolutions were found to evolve with a quantum yield of 5.9% in the range of 420-400 nm.

A Z-scheme system has been designed for overall water splitting into H_2 and O_2 using a two-step photoexcitation (R. Abe, et al., 2001). It was composed of an IO_3^-/I^- shuttle redox mediator and two different photocatalysts: Pt-loaded anatase TiO_2 for H_2 evolution and rutile TiO_2 for O_2 evolution. Under UV irradiation, simultaneous gas evolution of H_2 (180 μmol/h) and O_2 (90 μmol/h) was observed from a basic (pH=11) NaI aqueous suspension of these two different TiO_2 photocatalysts. The advantage of this system was that H_2 gas was evolved only over the Pt-TiO_2-anatase photocatalyst and that O_2 gas was evolved over the

TiO_2-rutile photocatalyst only, even from a mixture of IO_3^- and I^- in a basic aqueous solution. Therefore, the undesirable backward reaction, H_2O formation from H_2 and O_2 on Pt particles, was suppressed. Among the various Z-scheme systems studied, the (Pt/ZrO_2-TaON)-(Pt/WO_3)-(IO_3^-/I^-) system showed the highest photocatalytical activity for overall water splitting with a quantum efficiency of ca. 6.3% at 420.5 nm (X. B. Chen, et al., 2010). In this Z-scheme overall water splitting system, the H_2 and IO_3^- production took place over the Pt/ZrO_2-TaON photocatalyst; meanwhile, the IO_3^- reduction and water oxidation to O_2 took place over Pt-WO_3 under visible-light irradiation (K. Maeda, et al., 2010).
An overall water-splitting system driven by a Z-scheme inter-particle electron transfer between H_2 and O_2 photocatalysts (Ru/SrTiO3:Rh-BiVO4) without a redox mediator is shown in **Fig.8** (Y. Sasaki, et al., 2009). The undesirable reactions and negative effects by an electron mediator were excluded. Although the activity of a Z-scheme overall water splitting system is quite low and only a little higher than that achieved by conventional pure water-splitting systems using one single photocatalyst, these results provided a promising approach to constructing efficient overall water splitting systems.

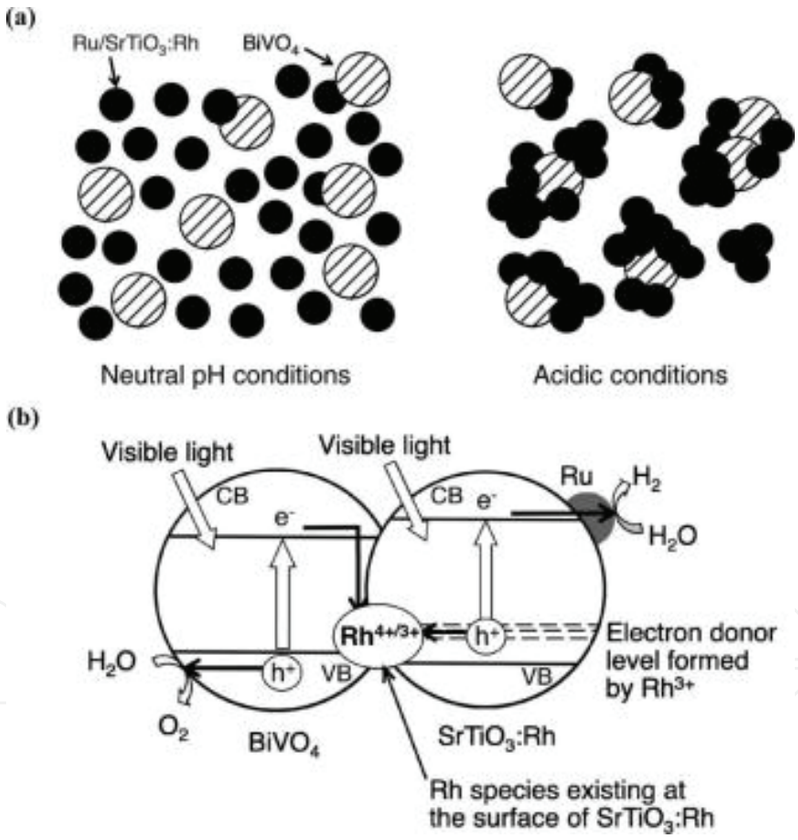

Fig. 8. Z-scheme water splitting without a redox mediator.

In summary, the research directions in solar hydrogen production via water splitting includes: (1) standardization of the photocatalyst characterization (Z. B. Chen, et al., 2010), (2) development of efficient narrow band gap semiconductors for visible light harvest (Z. B. Chen, et al., 2010; R. Dom, et al., 2011; J. H. Ye, et al., 2002), (3) construction of nanocomposites to enhance photogenerated charge separation and transfer (L. Amirav & A.

P. Alivisatos, 2010; J. Hensel, G. M. Wang, et al., 2010; H. Tada, et al., 2006), improve energy conversion efficiency (Y. L. Lee & Y. S. Lo, 2009), and realize hydrogen evolution reaction (M. Bar, et al., 2010), (4) development of inexpensive, effective and stable catalyst for HER and OER (M. G. Walter, et al., 2010) and to host them in well defined and tailored locations, (5) establishment of nanostructures to control charge movement and light absorption pathways which might allow the use of less expensive catalyst with lowered catalytic activities (X. B. Chen & S. S. Mao, 2006; E. Thimsen, et al., 2011; M. G. Walter, et al., 2010), and (6) improvement of the efficiency of the overall water splitting systems (K. Maeda, et al., 2008; K. Maeda, et al., 2010) through a better understanding of the reaction kinetics and carry out of scale-up study from lab to industry applications.

5. Photocatalytic degradation for cleanup of water and air, generation of electricity and hydrogen

Presently, the available efficiency for water splitting for simultaneous hydrogen and oxygen production under visible-light irradiation is still quite low due to fast charge recombination and backward reactions. To achieve enhanced and sustainable hydrogen production, the continual addition of electron donors is required to make up half of the water-splitting reaction to reduce H_2O to H_2. These sacrificial electron donors can irreversibly consume photogenerated holes, thus prohibiting undesirable charge recombination. Lowering cost for solar-to-H_2 energy conversion, polluting byproduct from industries (e.g., H_2S from nature gas wells, azodyes) and low-cost renewable biomass from animals or plants are preferential sacrificial electron donors (e.g. bio-ethanol, organic acids, saccharides) in water-splitting (or even electricity generation(M. Antoniadou & P. Lianos, 2010)) systems (V. M. Daskalaki, et al., 2010; P. Lianos, 2010). At little or no cost, they could be exploited to accomplish both the tasks of hydrogen production and waste treatment and biomass reforming simultaneously (X. B. Chen, et al., 2010). Such an admirable goal for the practical application of water-splitting systems is especially interesting in light of worldwide energy and environmental concerns.

In photocatalytical degradation of molecules, the holes generation by the photon can react with surface adsorbed H_2O to produce $\cdot OH$ radicals (hydroxyl ions acts as hole scavengers assisting electro-hole separation and preventing recombination), or directly oxidize the molecules into their radicals. In aerated systems, the conduction band electrons are usually scavenged by O_2 to yield superoxide radical anions $\cdot O_2$. By this ways, both the O_2 and the molecules are activated. The subsequent radical reactions usually have low or no barriers, resulting in the facile oxidative degradation of the molecules. **Fig.9** illustrated the energy levels of semiconductors. We can see that some band gaps straddle the $\cdot O_2/O_2$ and $\cdot OH/OH^-$ potentials (TiO_2, SnO_2, ZnO and $KTaO_3$). TiO_2 has established itself as the so far most successful photocatalyst for heterogeneous photocatalytical degradation of organic wastes, because it is stable in most chemical environments, seems nontoxic, can be easily synthesized and deposited as thin mesoporous film by soft chemistry techniques, like the sol–gel process. In addition, it is commercially available at very reasonable prices. TiO_2 is used as white pigment in all kinds of products, ranging from paints to tooth pastes. ZnO is the second broadly studied semiconductor after TiO_2.

The strategies used to improve the properties for TiO_2 and other semiconductors for solar hydrogen production via water splitting should be applicable here to photocatalytical degradation of organic wastes, such as doping TiO_2 for visible absorption, nanocomposites

for improvement of charge separation and transfer, co-catalyst sensitization (C. C. Chen, et al., 2010; P. Lianos, 2010).

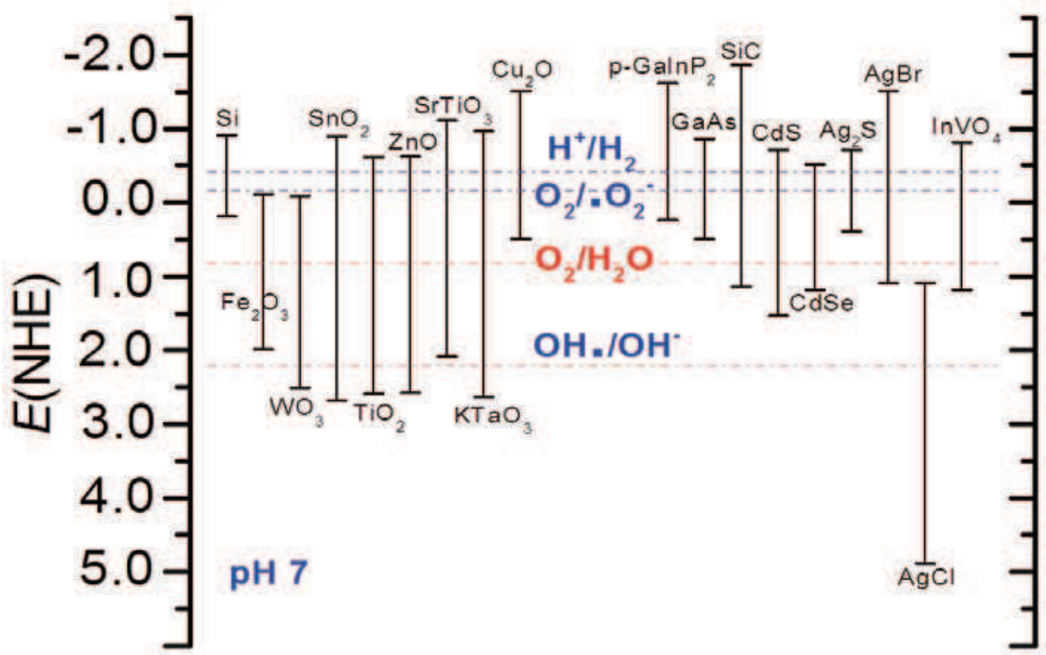

Fig. 9. Energetics of semiconductors at pH 7 for photocatalytical applications.

In the conventional photocatalysis process, the semiconductor is *directly excited* by light to initiate the degradation reaction (X. Chen & S. S. Mao, 2007; M. R. Hoffmann, et al., 1995; D. Ravelli, et al., 2009). However, a wide range of organic pollutants were found to be efficiently degraded on the surface of semiconductor, TiO_2, ZnO and others, via the ***electron injection*** of excited organic dyes or other color species (hence the name semiconductor-mediated photodegradation, SMPD (C. C. Chen, et al., 2010)). (1) Sensitizer degradation on dye-sensitized-semiconductor. Various organic *dye* pollutants have strong visible absorption, and themselves have been successfully degraded in the TiO_2 aqueous suspensions under visible irradiation (which is harvested by themselves) and in the presence of O_2 (T. X. Wu, et al., 1998). (2) Co-pollutants degradation by dye-sensitized-semiconductor. The organic radicals or active oxygen species formed using solar energy harvest by one kind of dye molecules can attack the other co-existing pollutants (dye, or pesticides that they might not need to harvest light by themselves) to drive their decontamination under visible light irradiation (D. Chatterjee & A. Mahata, 2001, 2004). (3) Pollutant degradation by QDots-sensitized-semiconductor. The surface modification by using more tolerant color species, such as inorganic metal complexes, noble metal nanoparticles and Qdots, can be conducted to construct stable photocatalysis systems, which are able to degrade even colorless pollutants under visible light irradiation, whereas color species themselves are regenerated and remain undegraded at the end of the degradation reaction (H. Kisch, et al., 1998; W. Zhao, et al., 2008). (4) The organic pollutants with appropriate redox potential (such as halogenated pollutants) can be reductively decontaminated by electrons injected into the conduction band (dehalogenation) (Y. M. Cho, et al., 2001; H. Kyung, et al., 2005).

Depositing an insulating Al_2O_3 shell (nanometers thick) on TiO_2 resulted in a significant retardation in the charge recombination dynamics (up to a 10-fold) (J. R. Durrant, et al., 2006). The rate constant for the SMPD of RhB in an Al_2O_3-modified TiO_2 system was nearly five-fold higher than that on pure TiO_2 (D. Zhao, et al., 2008). Very recently showed that introducing a thin Al_2O_3 layer on TiO_2 enhanced the visible light activities for the dechlorination of CCl_4 (W. Kim, et al., 2009). Measurements of time-resolved diffuse reflectance spectra of bare TiO_2 and Al_2O_3/TiO_2 in suspensions observed an increase in the average lifetime of the separated charges by about 3 times in Al_2O_3/TiO_2. In these systems, the dyes (RhB or Ruthenium bipyridyl complexes with carboxylate anchoring groups) were preferably adsorbed on the Al_2O_3, and the electrons injected into the TiO_2 by tunneling through the porous Al_2O_3 layer. On the other hand, the presence of the Al_2O_3 layer increases the physical separation between the injected electrons and the oxidized dye, thereby retarding the charge recombination reactions. But, the electron acceptors (such as O_2 and CCl_4) are still able to scavenge the conduction band electrons.

Silver nanoparticles have plasmon resonance absorption in the visible region. Irradiation on silver nanoparticles with various sizes and shapes on TiO_2 by a monochromatic visible light caused selective removal of the Ag particles due to the selective Plasmon absorption of the nanoparticles (Y. Ohko, et al., 2003). Ag nanoparticles were loaded on the surface of AgCl to constitute a plasmon-based photocatalyst with strong absorption in the visible region, and methyl orange dye was decomposed very rapidly under visible light irradiation on this plasmonic photocatalyst (P. Wang, et al., 2008). Au-deposited TiO_2 has been reported to exhibit enhanced photodegradation of Methylene Blue under visible light irradiation because of the increased absorption in the visible range (X. Z. Li & F. B. Li, 2001).

Combining TiO_2 with carbonaceous nanomaterials is being increasingly investigated as a means to increase photocatalytical activity, and demonstrations of enhancement are plentiful, which was reviewed recently on nanocarbon-TiO_2 photocatalysts, covering activated carbon, carbon doping, carbon nanotubes, [60]-fullerenes, graphene, thin layer carbon coating, nanometric carbon black and more recently developed morphologies. Mechanisms of enhancement, synthesis routes and future applications are summarized and discussed. New insight and enhanced photocatalytical activity may be provided by novel nanocarbon-TiO_2 systems (R. Leary & A. Westwood, 2011).

One approach to achieve visible light photo activity is to couple TiO_2 by a narrow band gap semiconductor such as CdS, $InVO_4$ (**Fig.9**). Visible-light-activated photocatalytical $Ag/InVO_4$-TiO_2 thin films were developed through a sol-gel method from the TiO_2 sol containing Ag and InVO4. The photocatalytical activities of $Ag/InVO_4$-TiO_2 thin films were investigated based on the oxidation decomposition of methyl orange in aqueous solution. The Ag and $InVO_4$ co-doped thin films significantly enhanced the methyl orange photodegradation under visible light irradiation (L. Ge, et al., 2006).

The visible light photocatalytical activities of platinized WO_3 (Pt/WO_3) was studied on the degradation of aquatic pollutants and the role of main photooxidants. The presence of Pt on WO_3 is known to facilitate the *multi-electron* reduction of O_2, which enables O_2 to serve as an electron acceptor despite the insufficient reduction potential of the conduction band electrons in WO_3 for the one-electron reduction of O_2 (cf. **Fig.9**). The concurrent oxidative reactions occurring on WO_3 were markedly enhanced in the presence of Pt and accompanied the production of OH radicals under visible light, which was confirmed by both a fluorescence method (using a chemical trap) and a spin trap method. The generation of OH

radicals mainly comes from the reductive decomposition of H_2O_2 that is produced in situ from the reduction of O_2 on Pt/ WO_3. The rate of in situ production of H_2O_2 under visible light was significantly faster with Pt/ WO_3 than WO_3. Six substrates that were tested for the visible light ($\lambda > 420$ nm) induced degradation on Pt/ WO_3 included dichloroacetate (DCA), 4-chlorophenol (4-CP), tetramethylammonium (TMA), arsenite (As(111)), methylene blue (MB), and acid orange 7 (A07). The degradation (or conversion) of all six substrates was successfully achieved with Pt/ WO_3 and the role of OH radicals in Pt/ WO_3 photocatalysis seemed to be different depending on the kind of substrate. In the presence of tert-butyl alcohol (TBA: OH radical scavenger), the photocatalytical degradation was markedly reduced for 4-CP or completely inhibited for DCA and TMA whereas that of As(III), MB, and A07 was little affected. Pt/WO_3 photocatalyst that oxidizes various substrates under visible light with a sufficient photostability can be applied for solar water treatment (J. Kim, et al., 2010).

The photocatalytical decomposition of acetaldehyde over $CaFe_2O_4$ (CFO)/WO_3 based composite photocatalysts under visible light irradiation was carried out. The photocatalytical activity of WO_3 was improved by simply mixing with CFO, and 5 wt % CFO coupled WO_3 showed the optimized performance. Ag and ITO coating on the CFO particle surface obviously promoted the photocatalytical activity of the CFO/WO_3 composite. The CFO/Ag (or ITO)/WO_3 composite photocatalyst could completely decompose acetaldehyde under visible light irradiation (Z. F. Liu, et al., 2009).

A review of patents on the application of titanium dioxide photocatalysis for air treatment was presented (Y. Paz, 2011). A comparison between water treatment and air treatment reveals that the number of scientific publications dedicated to photocatalytical air treatment is significantly lower than the number of scientific manuscripts dedicated to photocatalytical water treatment, yet the situation is reversed upon comparing relevant patents. This indicates a growing interest in the implementation of photocatalysis for air treatment purposes, which surpasses that of water treatment. The review analyzed the various patents in the area of air treatment, while differentiating between indoor air treatment and outdoor air treatment. Specific efforts were made to characterize the main challenges and achievements en-route for successful implementation, which were categorized according to mass transport, adsorption of contaminants, quantum efficiency, deactivation, and, no less important, the adherence and the long term stability of the photocatalyst.

In summary, future research in photocatalytical degradation should include, (1) systematic study on visible and solar light activated photocatalysts to achieve high efficiency (S. Ahmed, et al., 2010; C. C. Chen, et al., 2010), (2) catalyst immobilization strategy to provide cost-effective solid-liquid separation (M. N. Chong, et al., 2010; R. Leary & A. Westwood, 2011), (3) improvement in the photocatalytical operation for wider pH range, and (4) effective design of photocatalytical reaction system.

6. Conclusion

The discovery and utilization of solar composite materials have a long history which was dated back to 1800s. Accelerated development has taken place in recent decades, with a great promise to solve the global energy, environmental and social problems. Along with the relative maturing of dye sensitized solar cells, quantum dots solar energy harvesting is predicted to be the future technology to be developed, in the forms of QDSSC, solar hydrogen production via water splitting, and photocatalytical degradation of pollutants or

biomass in conjunction with fuel or electricity generation. In the effort to improve device efficiency and achieve commercialization, further research should be carried on to tailor the nanostructures, to control the charge separation and transportation, to effectively use inexpensive cocatalysts, and to study the reaction kinetics and their large scale realization.

7. References

Abe, R., Sayama, K., Domen, K., & Arakawa, H. (2001). A New Type of Water Splitting System Composed of Two Different Tio2 Photocatalysts (Anatase, Rutile) and a Io3-/I- Shuttle Redox Mediator. *Chemical Physics Letters*, Vol. 344, No. 3-4, pp. 339-344, 0009-2614.

Ahmed, S., Rasul, M. G., Martens, W. N., Brown, R., & Hashib, M. A. (2010). Heterogeneous Photocatalytic Degradation of Phenols in Wastewater: A Review on Current Status and Developments. *Desalination*, Vol. 261, No. 1-2, pp. 3-18, 0011-9164.

Alenzi, N., Liao, W. S., Cremer, P. S., Sanchez-Torres, V., Wood, T. K., Ehlig-Economides, C., et al. (2010). Photoelectrochemical Hydrogen Production from Water/Methanol Decomposition Using Ag/Tio2 Nanocomposite Thin Films. *International Journal of Hydrogen Energy*, Vol. 35, No. 21, pp. 11768-11775, 0360-3199.

Ameen, S., Akhtar, M. S., Kim, G. S., Kim, Y. S., Yang, O. B., & Shin, H. S. (2009). Plasma-Enhanced Polymerized Aniline/Tio2 Dye-Sensitized Solar Cells. *Journal of Alloys and Compounds*, Vol. 487, No. 1-2, pp. 382-386, 0925-8388.

Amirav, L., & Alivisatos, A. P. (2010). Photocatalytic Hydrogen Production with Tunable Nanorod Heterostructures. *Journal of Physical Chemistry Letters*, Vol. 1, No. 7, pp. 1051-1054, 1948-7185.

Antoniadou, M., & Lianos, P. (2010). Production of Electricity by Photoelectrochemical Oxidation of Ethanol in a Photofuelcell. *Applied Catalysis B-Environmental*, Vol. 99, No. 1-2, pp. 307-313, 0926-3373.

Bach, U., Lupo, D., Comte, P., Moser, J. E., Weissortel, F., Salbeck, J., et al. (1998). Solid-State Dye-Sensitized Mesoporous Tio2 Solar Cells with High Photon-to-Electron Conversion Efficiencies. *Nature*, Vol. 395, No. 6702, pp. 583-585, 0028-0836.

Baker, D. R., & Kamat, P. V. (2009). Photosensitization of Tio2 Nanostructures with Cds Quantum Dots: Particulate Versus Tubular Support Architectures. *Advanced Functional Materials*, Vol. 19, No. 5, pp. 805-811, 1616-301X.

Bang, J. H., & Kamat, P. V. (2009). Quantum Dot Sensitized Solar Cells. A Tale of Two Semiconductor Nanocrystals: Cdse and Cdte. *Acs Nano*, Vol. 3, No. 6, pp. 1467-1476, 1936-0851.

Bao, N., Shen, L., Takata, T., Domen, K., Gupta, A., & Yanagisawa, K. (2007). Facile Cd-Thiourea Complex Thermolysis Synthesis of Phase-Controlled Cds Nanocrystals for Photocatalytic Hydrogen Production under Visible Light. *Journal of Physical Chemistry C*, Vol. 111, No, pp. 17527-17534.

Bao, N. Z., Shen, L. M., Takata, T., & Domen, K. (2008). Self-Templated Synthesis of Nanoporous Cds Nanostructures for Highly Efficient Photocatalytic Hydrogen Production under Visible. *Chemistry of Materials*, Vol. 20, No. 1, pp. 110-117, 0897-4756.

Bar, M., Weinhardt, L., Marsen, B., Cole, B., Gaillard, N., Miller, E., et al. (2010). Mo Incorporation in Wo3 Thin Film Photoanodes: Tailoring the Electronic Structure for

Photoelectrochemical Hydrogen Production. *Applied Physics Letters*, Vol. 96, No. 3, pp. 032107, 0003-6951.

Barea, E. M., Shalom, M., Gimenez, S., Hod, I., Mora-Sero, I., Zaban, A., et al. (2010). Design of Injection and Recombination in Quantum Dot Sensitized Solar Cells. *Journal of the American Chemical Society*, Vol. 132, No. 19, pp. 6834-6839, 0002-7863.

Belaidi, A., Dittrich, T., Kieven, D., Tornow, J., Schwarzburg, K., & Lux-Steiner, M. (2008). Influence of the Local Absorber Layer Thickness on the Performance of Zno Nanorod Solar Cells. *Physica Status Solidi-Rapid Research Letters*, Vol. 2, No. 4, pp. 172-174, 1862-6254.

Biello, D. (2008). Inside the Solar-Hydrogen House: No More Power Bills--Ever. *Scientific American*. Retrieved from http://www.scientificamerican.com/article.cfm?id=hydrogen-house

Bolton, J. R., Strickler, S. J., & Connolly, J. S. (1985). Limiting and Realizable Efficiencies of Solar Photolysis of Water. *Nature*, Vol. 316, No. 6028, pp. 495-500, 0028-0836.

Bonde, J., Moses, P. G., Jaramillo, T. F., Norskov, J. K., & Chorkendorff, I. (2008). Hydrogen Evolution on Nano-Particulate Transition Metal Sulfides. *Faraday Discussions*, Vol. 140, No, pp. 219-231, 1364-5498.

Bosi, M., & Pelosi, C. (2007). The Potential of Iii-V Semiconductors as Terrestrial Photovoltaic Devices. *Progress in Photovoltaics*, Vol. 15, No. 1, pp. 51-68, 1062-7995.

Boumaza, S., Boudjemaa, A., Bouguelia, A., Bouarab, R., & Trari, M. (2010). Visible Light Induced Hydrogen Evolution on New Hetero-System Znfe2o4/Srtio3. *Applied Energy*, Vol. 87, No. 7, pp. 2230-2236, 0306-2619.

Brattain, W. H., & Garrett, C. G. B. (1955). Experiments on the Interface between Germanium and an Electrolyte. *Bell System Technical Journal*, Vol. 34, No. 1, pp. 129-176, 0005-8580.

Brillet, J., Gratzel, M., & Sivula, K. (2010). Decoupling Feature Size and Functionality in Solution-Processed, Porous Hematite Electrodes for Solar Water Splitting. *Nano Letters*, Vol. 10, No. 10, pp. 4155-4160, 1530-6984.

Carlson, D. E., & Wronski, C. R. (1976). Amorphous Silicon Solar-Cell. *Applied Physics Letters*, Vol. 28, No. 11, pp. 671-673, 0003-6951.

Cesar, I., Sivula, K., Kay, A., Zboril, R., & Graetzel, M. (2009). Influence of Feature Size, Film Thickness, and Silicon Doping on the Performance of Nanostructured Hematite Photoanodes for Solar Water Splitting. *Journal of Physical Chemistry C*, Vol. 113, No. 2, pp. 772-782, 1932-7447.

Chapin, D. M., Fuller, C. S., & Pearson, G. L. (1954). A New Silicon P-N Junction Photocell for Converting Solar Radiation into Electrical Power. *Journal of Applied Physics*, Vol. 25, No. 5, pp. 676-677, 0021-8979.

Chatterjee, D., & Mahata, A. (2001). Demineralization of Organic Pollutants on the Dye Modified Tio2 Semiconductor Particulate System Using Visible Light. *Applied Catalysis B-Environmental*, Vol. 33, No. 2, pp. 119-125, 0926-3373.

Chatterjee, D., & Mahata, A. (2004). Evidence of Superoxide Radical Formation in the Photodegradation of Pesticide on the Dye Modified Tio2 Surface Using Visible Light. *Journal of Photochemistry and Photobiology a-Chemistry*, Vol. 165, No. 1-3, pp. 19-23, 1010-6030.

Chen, Z.B., Kibsgaard, J. & Jaramillo, T.F., (2010) Nanostructuring MoS2 for Photoelectrochemical Water Splitting. *Solar Hydrogen and Nanotechnology V,*

Proceedings of the SPIE-The International Society for Optical Engieering, Vol 7770, pp 7770-K1-K7,0277-768X

Chen, C. C., Ma, W. H., & Zhao, J. C. (2010). Semiconductor-Mediated Photodegradation of Pollutants under Visible-Light Irradiation. *Chemical Society Reviews*, Vol. 39, No. 11, pp. 4206-4219, 0306-0012.

Chen, J., Zhao, D. W., Song, J. L., Sun, X. W., Deng, W. Q., Liu, X. W., et al. (2009). Directly Assembled Cdse Quantum Dots on Tio2 in Aqueous Solution by Adjusting Ph Value for Quantum Dot Sensitized Solar Cells. *Electrochemistry Communications*, Vol. 11, No. 12, pp. 2265-2267, 1388-2481.

Chen, X., & Mao, S. S. (2007). Titanium Dioxide Nanomaterials: Synthesis, Properties, Modifications, and Applications. *Chemical Reviews*, Vol. 107, No. 7, pp. 2891-2959, 0009-2665.

Chen, X. B., Lou, Y. B., Samia, A. C. S., Burda, C., & Gole, J. L. (2005). Formation of Oxynitride as the Photocatalytic Enhancing Site in Nitrogen-Doped Titania Nanocatalysts: Comparison to a Commercial Nanopowder. *Advanced Functional Materials*, Vol. 15, No. 1, pp. 41-49, 1616-301X.

Chen, X. B., & Mao, S. S. (2006). Synthesis of Titanium Dioxide (Tio2) Nanomaterials. *Journal of Nanoscience and Nanotechnology*, Vol. 6, No. 4, pp. 906-925, 1533-4880.

Chen, X. B., Shen, S. H., Guo, L. J., & Mao, S. S. (2010). Semiconductor-Based Photocatalytic Hydrogen Generation. *Chemical Reviews*, Vol. 110, No. 11, pp. 6503-6570, 0009-2665.

Chen, Z. B., Jaramillo, T. F., Deutsch, T. G., Kleiman-Shwarsctein, A., Forman, A. J., Gaillard, N., et al. (2010). Accelerating Materials Development for Photoelectrochemical Hydrogen Production: Standards for Methods, Definitions, and Reporting Protocols. *Journal of Materials Research*, Vol. 25, No. 1, pp. 3-16, 0884-2914.

Chianelli, R. R., Siadati, M. H., De la Rosa, M. P., Berhault, G., Wilcoxon, J. P., Bearden, R., et al. (2006). Catalytic Properties of Single Layers of Transition Metal Sulfide Catalytic Materials. *Catalysis Reviews-Science and Engineering*, Vol. 48, No. 1, pp. 1-41, 0161-4940.

Cho, Y. M., Choi, W. Y., Lee, C. H., Hyeon, T., & Lee, H. I. (2001). Visible Light-Induced Degradation of Carbon Tetrachloride on Dye-Sensitized Tio2. *Environmental Science & Technology*, Vol. 35, No. 5, pp. 966-970, 0013-936X.

Cho, Y. M., & Choi, W. Y. (2002). Visible Light-Induced Reactions of Humic Acids on Tio2. *Journal of Photochemistry and Photobiology a-Chemistry*, Vol. 148, No. 1-3, pp. 129-135, 1010-6030.

Chong, M. N., Jin, B., Chow, C. W. K., & Saint, C. (2010). Recent Developments in Photocatalytic Water Treatment Technology: A Review. *Water Research*, Vol. 44, No. 10, pp. 2997-3027, 0043-1354.

Combs, S. (2008). The Energy Report (Chapter 22). Retrieved from http://window.state.tx.us/specialrpt/energy

Contreras, M. A., Egaas, B., Ramanathan, K., Hiltner, J., Swartzlander, A., Hasoon, F., et al. (1999). Progress toward 20% Efficiency in Cu(in,Ca)Se-2 Polycrystalline Thin-Film Solar Cells. *Progress in Photovoltaics*, Vol. 7, No. 4, pp. 311-316, 1062-7995.

Crabtree, G. W., Dresselhaus, M. S., & Buchanan, M. V. (2004). The Hydrogen Economy. *Physics Today*, Vol. 57, No. 12, pp. 39-44, 0031-9228.

Currao, A. (2007). Photoelectrochemical Water Splitting. *CHIMIA International Journal for Chemistry*, Vol. 61, No, pp. 815-819.

Daskalaki, V. M., Antoniadou, M., Puma, G. L., Kondarides, D. I., & Lianos, P. (2010). Solar Light-Responsive Pt/Cds/Tio2 Photocatalysts for Hydrogen Production and Simultaneous Degradation of Inorganic or Organic Sacrificial Agents in Wastewater. *Environmental Science & Technology*, Vol. 44, No. 19, pp. 7200-7205, 0013-936X.

Derbal, A., Omeiri, S., Bouguelia, A., & Trari, M. (2008). Characterization of New Heterosystem Cufeo2/Sno2 Application to Visible-Light Induced Hydrogen Evolution. *International Journal of Hydrogen Energy*, Vol. 33, No. 16, pp. 4274-4282, 0360-3199.

DeVos, A. (1980). Detailed Balance Limit of the Efficiency of Tandem Solar Cells. *Journal of Physics D: Applied Physics*, Vol. 13, No. 5, pp. 839-846.

Diguna, L. J., Shen, Q., Kobayashi, J., & Toyoda, T. (2007a). High Efficiency of Cdse Quantum-Dot-Sensitized Tio2 Inverse Opal Solar Cells. *Applied Physics Letters*, Vol. 91, No. 2, pp. 023116, 0003-6951.

Diguna, L. J., Shen, Q., Kobayashi, J., & Toyoda, T. (2007b). High Efficiency of Cdse Quantum-Dot-Sensitized Tio2 Inverse Opal Solar Cells. *Applied Physics Letters*, Vol. 91, No. 2, pp, 0003-6951.

Dom, R., Subasri, R., Radha, K., & Borse, P. H. (2011). Synthesis of Solar Active Nanocrystalline Ferrite, Mfe2o4 (M: Ca, Zn, Mg) Photocatalyst by Microwave Irradiation. *Solid State Communications*, Vol. 151, No. 6, pp. 470-473, 0038-1098.

Dougherty, W., Kartha, S., Rajan, C., Lazarus, M., Bailie, A., Runkle, B., et al. (2009). Greenhouse Gas Reduction Benefits and Costs of a Large-Scale Transition to Hydrogen in the USA. *Energy Policy*, Vol. 37, No. 1, pp. 56-67, 0301-4215.

Durrant, J. R., Haque, S. A., & Palomares, E. (2006). Photochemical Energy Conversion: From Molecular Dyads to Solar Cells. *Chemical Communications*, Vol. 31, pp. 3279-3289, 1359-7345.

Frame, F. A., & Osterloh, F. E. (2010). Cdse-Mos2: A Quantum Size-Confined Photocatalyst for Hydrogen Evolution from Water under Visible Light. *Journal of Physical Chemistry C*, Vol. 114, No. 23, pp. 10628-10633, 1932-7447.

Fujishima, A., & Honda, K. (1972). Electrochemical Photolysis of Water at a Semiconductor Electrode. *Nature*, Vol. 238, No, pp. 37-38.

Fujishima, A., & Honda, K. (1972). Electrochemical Photolysis of Water at a Semiconductor Electrode. *Nature*, Vol. 238, No. 5358, pp. 37-38, 0028-0836.

Gaillard, N., Kaneshiro, J., Miller, E. L., Weinhardt, L., Bar, M., Heske, C., et al. (2009). Surface Modification of Tungsten Oxide-Based Photoanodes for Solar-Powered Hydrogen Production. In *Compound Semiconductors for Energy Applications and Environmental Sustainability*, ShahedipourSandvik, F., Schubert, E. F., Bell, L. D., Tilak, V. & Bett, A. W. (Eds.), (Vol. 1167), pp. 109-114 Materials Research Society, 0272-9172, Warrendale.

Gaillard, N., Chang, Y., Kaneshiro, J., Deangelis, A., & Miller, E. L. (2010). Status of Research on Tungsten Oxide-Based Photoelectrochemical Devices at the University of Hawai'i. In *Solar Hydrogen and Nanotechnology V*, Idriss, H. & Wang, H. (Eds.), (Vol. 7770), pp. 77700V-77701, 0277-786X 978-0-8194-8266-2.

Ge, L., Xu, M. X., & Fang, H. B. (2006). Preparation and Characterization of Silver and Indium Vanadate Co-Doped Tio2 Thin Films as Visible-Light-Activated

Photocatalyst. *Journal of Sol-Gel Science and Technology*, Vol. 40, No. 1, pp. 65-73, 0928-0707.

Gerische, H. (1966). Electrochemical Behavior of Semiconductors under Illumination. *Journal of the Electrochemical Society*, Vol. 113, No. 11, pp. 1174-1182, 0013-4651.

Gimenez, S., Mora-Sero, I., Macor, L., Guijarro, N., Lana-Villarreal, T., Gomez, R., et al. (2009). Improving the Performance of Colloidal Quantum-Dot-Sensitized Solar Cells. *Nanotechnology*, Vol. 20, No. 29, pp, 0957-4484.

Goncalves, L. M., Bermudez, V. D., Ribeiro, H. A., & Mendes, A. M. (2008). Dye-Sensitized Solar Cells: A Safe Bet for the Future. *Energy & Environmental Science*, Vol. 1, No. 6, pp. 655-667, 1754-5692.

Gonzalez-Pedro, V., Xu, X. Q., Mora-Sero, I., & Bisquert, J. (2010). Modeling High-Efficiency Quantum Dot Sensitized Solar Cells. *Acs Nano*, Vol. 4, No. 10, pp. 5783-5790, 1936-0851.

Gorer, S., & Hodes, G. (1994). Quantum-Size Effects in the Study of Chemical Solution Deposition Mechanisms of Semiconductor-Films. *Journal of Physical Chemistry*, Vol. 98, No. 20, pp. 5338-5346, 0022-3654.

Granqvist, C. G. (2000). Electrochromic Tungsten Oxide Films: Review of Progress 1993-1998. *Solar Energy Materials and Solar Cells*, Vol. 60, No. 3, pp. 201-262, 0927-0248.

Gratzel, M. (2001). Photoelectrochemical Cells. *Nature*, Vol. 414, No. 6861, pp. 338-344, 0028-0836.

Gratzel, M. (2004). Conversion of Sunlight to Electric Power by Nanocrystalline Dye-Sensitized Solar Cells. *Journal of Photochemistry and Photobiology a-Chemistry*, Vol. 164, No. 1-3, pp. 3-14, 1010-6030.

Gratzel, M. (2007). Photovoltaic and Photoelectrochemical Conversion of Solar Energy. *Philosophical Transactions of the Royal Society a-Mathematical Physical and Engineering Sciences*, Vol. 365, No. 1853, pp. 993-1005, 1364-503X.

Green, M. A. (2003). *Third Generation Photovoltaics: Advanced Solar Energy Conversion*, Springer-Verlag, Berlin, Heidelberg.

Green, M. A., Emery, K., Hishikawa, Y., & Warta, W. (2008). Solar Cell Efficiency Tables (Version 32). *Progress in Photovoltaics*, Vol. 16, No. 5, pp. 435-440, 1062-7995.

Guijarro, N., Lana-Villarreal, T., Mora-Sero, I., Bisquert, J., & Gomez, R. (2009). Cdse Quantum Dot-Sensitized Tio2 Electrodes: Effect of Quantum Dot Coverage and Mode of Attachment. *Journal of Physical Chemistry C*, Vol. 113, No. 10, pp. 4208-4214, 1932-7447.

Gunes, S., & Sariciftci, N. S. (2008). Hybrid Solar Cells. *Inorganica Chimica Acta*, Vol. 361, No, pp. 581-588.

Hagfeldt, A., Boschloo, G., Sun, L. C., Kloo, L., & Pettersson, H. (2010). Dye-Sensitized Solar Cells. *Chemical Reviews*, Vol. 110, No. 11, pp. 6595-6663, 0009-2665.

Hauffe, K., Danzmann, H. J., Pusch, H., Range, J., & Volz, H. (1970). New Experiments on Sensitization of Zinc Oxide by Means of Electrochemical Cell Technique. *Journal of the Electrochemical Society*, Vol. 117, No. 8, pp. 993-999, 0013-4651.

Heller, A. (1981). Conversion of Sunlight into Electrical-Power and Photoassisted Electrolysis of Water in Photoelectrochemical Cells. *Accounts of Chemical Research*, Vol. 14, No. 5, pp. 154-162, 0001-4842.

Hensel, J., Canin, M., & Zhang, J. Z. (2010). Qd Co-Sensitized and Nitrogen Doped Tio2 Nanocomposite for Photoelectrochemical Hydrogen Generation. In *Solar Hydrogen*

and Nanotechnology V, Idriss, H. & Wang, H. (Eds.), (Vol. 7770), pp. 777012 Spie-Int Soc Optical Engineering, 0277-786X 978-0-8194-8266-2, Bellingham.

Hensel, J., Wang, G. M., Li, Y., & Zhang, J. Z. (2010). Synergistic Effect of Cdse Quantum Dot Sensitization and Nitrogen Doping of Tio2 Nanostructures for Photoelectrochemical Solar Hydrogen Generation. *Nano Letters*, Vol. 10, No. 2, pp. 478-483, 1530-6984.

Hodes, G., Cahen, D., & Manassen, J. (1976). Tungsten Trioxide as a Photoanode for a Photoelectrochemical Cell (Pec). *Nature*, Vol. 260, No. 5549, pp. 312-313, 0028-0836.

Hodes, G. (2008). Comparison of Dye- and Semiconductor-Sensitized Porous Nanocrystalline Liquid Junction Solar Cells. *Journal of Physical Chemistry C*, Vol. 112, No. 46, pp. 17778-17787, 1932-7447.

Hoffmann, M. R., Martin, S. T., Choi, W. Y., & Bahnemann, D. W. (1995). Environmental Applications of Semiconductor Photocatalysis. *Chemical Reviews*, Vol. 95, No. 1, pp. 69-96, 0009-2665.

Hu, C. C., Nian, J. N., & Teng, H. (2008). Electrodeposited P-Type Cu2o as Photocatalyst for H-2 Evolution from Water Reduction in the Presence of Wo3. *Solar Energy Materials and Solar Cells*, Vol. 92, No. 9, pp. 1071-1076, 0927-0248.

Huang, S. Q., Zhang, Q. X., Huang, X. M., Guo, X. Z., Deng, M. H., Li, D. M., et al. (2010). Fibrous Cds/Cdse Quantum Dot Co-Sensitized Solar Cells Based on Ordered Tio2 Nanotube Arrays. *Nanotechnology*, Vol. 21, No. 37, pp. 375201, 0957-4484.

Ikeda, N., & Miyasaka, T. (2007). Plastic and Solid-State Dye-Sensitized Solar Cells Incorporating Single-Wall Carbon Nanotubes. *Chemistry Letters*, Vol. 36, No. 3, pp. 466-467, 0366-7022.

Jang, J. S., Joshi, U. A., & Lee, J. S. (2007). Solvothermal Synthesis of Cds Nanowires for Photocatalytic Hydrogen and Electricity Production. *Journal of Physical Chemistry C*, Vol. 111, No, pp. 13280–13287.

Jaramillo, T. F., Jorgensen, K. P., Bonde, J., Nielsen, J. H., Horch, S., & Chorkendorff, I. (2007). Identification of Active Edge Sites for Electrochemical H-2 Evolution from Mos2 Nanocatalysts. *Science*, Vol. 317, No. 5834, pp. 100-102, 0036-8075.

Kalyanasundaram, K. (1985). Photoelectrochemical Cell Studies with Semiconductor Electrodes - a Classified Bibliography (1975 - 1983). *Solar Cells*, Vol. 15, No. 2, pp. 93-156, 0379-6787.

Kalyanasundaram, K., & Gratzel, M. (1998). Applications of Functionalized Transition Metal Complexes in Photonic and Optoelectronic Devices. *Coordination Chemistry Reviews*, Vol. 177, No, pp. 347-414, 0010-8545.

Kamat, P. V. (2007). Meeting the Clean Energy Demand: Nanostructure Architectures for Solar Energy Conversion. *Journal of Physical Chemistry C*, Vol. 111, No. 7, pp. 2834-2860, 1932-7447.

Kanda, S., Akita, T., Fujishima, M., & Tada, H. (2011). Facile Synthesis and Catalytic Activity of Mos2/Tio2 by a Photodeposition-Based Technique and Its Oxidized Derivative Moo3/Tio2 with a Unique Photochromism. *Journal of Colloid and Interface Science*, Vol. 354, No. 2, pp. 607-610, 0021-9797.

Kay, A., Cesar, I., & Gratzel, M. (2006). New Benchmark for Water Photooxidation by Nanostructured Alpha-Fe2o3 Films. *Journal of the American Chemical Society*, Vol. 128, No. 49, pp. 15714-15721, 0002-7863.

Kennedy, J. H., & Frese, K. W. (1977). Photooxidation of Water at Alpha-Fe2o3 Electrodes. *Journal of the Electrochemical Society*, Vol. 124, No. 3, pp. C130-C130, 0013-4651.

Kennedy, J. H., & Anderman, M. (1983). Photoelectrolysis of Water at Alpha-Fe2o3 Electrodes in Acidic Solution. *Journal of the Electrochemical Society*, Vol. 130, No. 4, pp. 848-852, 0013-4651.

Khan, S. U. M., & Akikusa, J. (1999). Photoelectrochemical Splitting of Water at Nanocrystalline N-Fe2o3 Thin-Film Electrodes. *Journal of Physical Chemistry B*, Vol. 103, No. 34, pp. 7184-7189, 1089-5647.

Khan, S. U. M., Al-Shahry, M., & Ingler, W. B. (2002). Efficient Photochemical Water Splitting by a Chemically Modified N-Tio2 2. *Science*, Vol. 297, No. 5590, pp. 2243-2245, 0036-8075.

Khaselev, O., & Turner, J. A. (1998a). A Monolithic Photovoltaic-Photoelectrochemical Device for Hydrogen Production Via Water Splitting. *Science*, Vol. 280, No. 5362, pp. 425-427, 0036-8075.

Khaselev, O., & Turner, J. A. (1998b). Electrochemical Stability of P-Gainp2 in Aqueous Electrolytes toward Photoelectrochemical Water Splitting. *Journal of the Electrochemical Society*, Vol. 145, No. 10, pp. 3335-3339, 0013-4651.

Khaselev, O., Bansal, A., & Turner, J. A. (2001). High-Efficiency Integrated Multijunction Photovoltaic/Electrolysis Systems for Hydrogen Production. *International Journal of Hydrogen Energy*, Vol. 26, No. 2, pp. 127-132, 0360-3199.

Kikuchi, E., Nemoto, Y., Kajiwara, M., Uemiya, S., & Kojima, T. (2000). Steam Reforming of Methane in Membrane Reactors: Comparison of Electroless-Plating and Cvd Membranes and Catalyst Packing Modes. *Catalysis Today*, Vol. 56, No. 1-3, pp. 75-81, 0920-5861.

Kim, J., Lee, C. W., & Choi, W. (2010). Platinized Wo3 as an Environmental Photocatalyst That Generates Oh Radicals under Visible Light. *Environmental Science & Technology*, Vol. 44, No. 17, pp. 6849-6854, 0013-936X.

Kim, J. Y., Lee, K., Coates, N. E., Moses, D., Nguyen, T. Q., Dante, M., et al. (2007). Efficient Tandem Polymer Solar Cells Fabricated by All-Solution Processing. *Science*, Vol. 317, No. 5835, pp. 222-225, 0036-8075.

Kim, W., Tachikawa, T., Majima, T., & Choi, W. (2009). Photocatalysis of Dye-Sensitized Tio2 Nanoparticles with Thin Overcoat of Al2o3: Enhanced Activity for H-2 Production and Dechlorination of Ccl4. *Journal of Physical Chemistry C*, Vol. 113, No. 24, pp. 10603-10609, 1932-7447.

Kisch, H., Zang, L., Lange, C., Maier, W. F., Antonius, C., & Meissner, D. (1998). Modified, Amorphous Titania - a Hybrid Semiconductor for Detoxification and Current Generation by Visible Light. *Angewandte Chemie-International Edition*, Vol. 37, No. 21, pp. 3034-3036, 1433-7851.

Klimov, V. I. (2006). Detailed-Balance Power Conversion Limits of Nanocrystal-Quantum-Dot Solar Cells in the Presence of Carrier Multiplication. *Applied Physics Letters*, Vol. 89, No. 12, pp. 123118, 0003-6951.

Kongkanand, A., Dominguez, R. M., & Kamat, P. V. (2007). Single Wall Carbon Nanotube Scaffolds for Photoelectrochemical Solar Cells. Capture and Transport of Photogenerated Electrons. *Nano Letters*, Vol. 7, No. 3, pp. 676-680, 1530-6984.

Kongkanand, A., Tvrdy, K., Takechi, K., Kuno, M., & Kamat, P. V. (2008). Quantum Dot Solar Cells. Tuning Photoresponse through Size and Shape Control of Cdse-Tio2

Architecture. *Journal of the American Chemical Society*, Vol. 130, No. 12, pp. 4007-4015, 0002-7863.

Kowalska, E., Mahaney, O. O. P., Abe, R., & Ohtani, B. (2010). Visible-Light-Induced Photocatalysis through Surface Plasmon Excitation of Gold on Titania Surfaces. *Physical Chemistry Chemical Physics*, Vol. 12, No. 10, pp. 2344-2355, 1463-9076.

Kyung, H., Lee, J., & Choi, W. Y. (2005). Simultaneous and Synergistic Conversion of Dyes and Heavy Metal Ions in Aqueous Tio2 Suspensions under Visible-Light Illumination. *Environmental Science & Technology*, Vol. 39, No. 7, pp. 2376-2382, 0013-936X.

Le Formal, F., Gratzel, M., & Sivula, K. (2010). Controlling Photoactivity in Ultrathin Hematite Films for Solar Water-Splitting. *Advanced Functional Materials*, Vol. 20, No. 7, pp. 1099-1107, 1616-301X.

Leary, R., & Westwood, A. (2011). Carbonaceous Nanomaterials for the Enhancement of Tio2 Photocatalysis. *Carbon*, Vol. 49, No. 3, pp. 741-772, 0008-6223.

Lee, H., Wang, M. K., Chen, P., Gamelin, D. R., Zakeeruddin, S. M., Gratzel, M., et al. (2009). Efficient Cdse Quantum Dot-Sensitized Solar Cells Prepared by an Improved Successive Ionic Layer Adsorption and Reaction Process. *Nano Letters*, Vol. 9, No. 12, pp. 4221-4227, 1530-6984.

Lee, H. J., Yum, J. H., Leventis, H. C., Zakeeruddin, S. M., Haque, S. A., Chen, P., et al. (2008). Cdse Quantum Dot-Sensitized Solar Cells Exceeding Efficiency 1% at Full-Sun Intensity. *Journal of Physical Chemistry C*, Vol. 112, No. 30, pp. 11600-11608, 1932-7447.

Lee, Y. L., & Lo, Y. S. (2009). Highly Efficient Quantum-Dot-Sensitized Solar Cell Based on Co-Sensitization of Cds/Cdse. *Advanced Functional Materials*, Vol. 19, No. 4, pp. 604-609, 1616-301X.

Levy-Clement, C., Tena-Zaera, R., Ryan, M. A., Katty, A., & Hodes, G. (2005). Cdse-Sensitized P-Cuscn/Nanowire N-Zno Heterojunctions. *Advanced Materials*, Vol. 17, No. 12, pp. 1512-1515, 0935-9648.

Lewis, N. S. (2001). Light Work with Water. *Nature*, Vol. 414, No, pp. 589-590.

Li, B., Wang, L. D., Kang, B. N., Wang, P., & Qiu, Y. (2006). Review of Recent Progress in Solid-State Dye-Sensitized Solar Cells. *Solar Energy Materials and Solar Cells*, Vol. 90, No. 5, pp. 549-573, 0927-0248.

Li, X. Z., & Li, F. B. (2001). Study of Au/Au3+-Tio2 Photocatalysts toward Visible Photooxidation for Water and Wastewater Treatment. *Environmental Science & Technology*, Vol. 35, No. 11, pp. 2381-2387, 0013-936X.

Li, Y., Hu, Y., Peng, S., Lu, G., & Li, S. (2009). Nanorods by an Ethylenediamine Assisted Hydrothermal Method for Photocatalytic Hydrogen Evolution. *Journal of Physical Chemistry C* Vol. 113, No, pp. 9352-9358.

Lianos, P. (2010). Production of Electricity and Hydrogen by Photocatalytic Degradation of Organic Wastes in a Photoelectrochemical Cell the Concept of the Photofuelcell: A Review of a Re-Emerging Research Field. *Journal of Hazardous Materials*, Vol. 185, No. 2-3, pp. 575-590, 0304-3894.

Lin, Y. J., Zhou, S., Liu, X. H., Sheehan, S., & Wang, D. W. (2009). Tio2/Tisi2 Heterostructures for High-Efficiency Photoelectrochemical H2o Splitting. *Journal of the American Chemical Society*, Vol. 131, No. 8, pp. 2772-2773, 0002-7863.

Liu, Z. F., Zhao, Z. G., & Miyauchi, M. (2009). Efficient Visible Light Active Cafe2o4/Wo3 Based Composite Photocatalysts: Effect of Interfacial Modification. *Journal of Physical Chemistry C*, Vol. 113, No. 39, pp. 17132-17137, 1932-7447.

Lopez-Luke, T., Wolcott, A., Xu, L. P., Chen, S. W., Wcn, Z. H., Li, J. H., et al. (2008). Nitrogen-Doped and Cdse Quantum-Dot-Sensitized Nanocrystalline Tio2 Films for Solar Energy Conversion Applications. *Journal of physical Chemistry C*, Vol. 112, No. 4, pp. 1282-1292, 1932-7447.

Maeda, K., Teramura, K., & Domen, K. (2008). Effect of Post-Calcination on Photocatalytic Activity of (Ga1-Xznx)(N1-Xox) Solid Solution for Overall Water Splitting under Visible Light. *Journal of Catalysis*, Vol. 254, No. 2, pp. 198-204, 0021-9517.

Maeda, K., Higashi, M., Lu, D. L., Abe, R., & Domen, K. (2010). Efficient Nonsacrificial Water Splitting through Two-Step Photoexcitation by Visible Light Using a Modified Oxynitride as a Hydrogen Evolution Photocatalyst. *Journal of the American Chemical Society*, Vol. 132, No. 16, pp. 5858-5868, 0002-7863.

Marti, A., & Araujo, G. L. (1996). Limiting Efficiencies for Photovoltaic Energy Conversion in Multigap Systems. *Solar Energy Materials and Solar Cells*, Vol. 43, No. 2, pp. 203-222, 0927-0248.

Matsuoka, M., Kitano, M., Takeuchi, M., Tsujimaru, K., Anpo, M., & Thomas, J. M. (2007). Photocatalysis for New Energy Production - Recent Advances in Photocatalytic Water Splitting Reactions for Hydrogen Production. *Catalysis Today*, Vol. 122, No. 1-2, pp. 51-61, 0920-5861.

Miller, E. L., Paluselli, D., Marsen, B., & Rocheleau, R. E. (2005). Development of Reactively Sputtered Metal Oxide Films for Hydrogen-Producing Hybrid Multijunction Photoelectrodes. *Solar Energy Materials and Solar Cells*, Vol. 88, No. 2, pp. 131-144, 0927-0248.

Mora-Sero, I., Gimenez, S., Moehl, T., Fabregat-Santiago, F., Lana-Villareal, T., Gomez, R., et al. (2008). Factors Determining the Photovoltaic Performance of a Cdse Quantum Dot Sensitized Solar Cell: The Role of the Linker Molecule and of the Counter Electrode. *Nanotechnology*, Vol. 19, No. 42, pp, 0957-4484.

Mora-Sero, I., & Bisquert, J. (2010). Breakthroughs in the Development of Semiconductor-Sensitized Solar Cells. *Journal of Physical Chemistry Letters*, Vol. 1, No. 20, pp. 3046-3052, 1948-7185.

Moreels, I., Lambert, K., De Muynck, D., Vanhaecke, F., Poelman, D., Martins, J. C., et al. (2007). Composition and Size-Dependent Extinction Coefficient of Colloidal Pbse Quantum Dots. *Chemistry of Materials*, Vol. 19, No. 25, pp. 6101-6106, 0897-4756.

Murakoshi, K., Kogure, R., Wada, Y., & Yanagida, S. (1998). Fabrication of Solid-State Dye-Sensitized Tio2 Solar Cells Combined with Polypyrrole. *Solar Energy Materials and Solar Cells*, Vol. 55, No. 1-2, pp. 113-125, 0927-0248.

Muratore, C., & Voevodin, A. A. (2009). Chameleon Coatings: Adaptive Surfaces to Reduce Friction and Wear in Extreme Environments. *Annual Review of Materials Research*, Vol. 39, No, pp. 297-324, 1531-7331.

Murphy, A. B., Barnes, P. R. F., Randeniya, L. K., Plumb, I. C., Grey, I. E., Horne, M. D., et al. (2006). Efficiency of Solar Water Splitting Using Semiconductor Electrodes. *International Journal of Hydrogen Energy*, Vol. 31, No. 14, pp. 1999-2017, 0360-3199.

Nazeeruddin, M. K., Pechy, P., Renouard, T., Zakeeruddin, S. M., Humphry-Baker, R., Comte, P., et al. (2001). Engineering of Efficient Panchromatic Sensitizers for

Nanocrystalline Tio2-Based Solar Cells. *Journal of the American Chemical Society*, Vol. 123, No. 8, pp. 1613-1624, 0002-7863.

Nelson, R. C. (1965). Minority Carrier Trapping and Dye Sensitization. *Journal of Physical Chemistry*, Vol. 69, No. 3, pp. 714-&, 0022-3654.

Ni, M., Leung, M. K. H., Leung, D. Y. C., & Sumathy, K. (2007). A Review and Recent Developments in Photocatalytic Water-Splitting Using Tio2 for Hydrogen Production. *Renewable and Sustainable Energy Reviews*, Vol. 11, No. 3, pp. 401-425, 1364-0321.

Niitsoo, O., Sarkar, S. K., Pejoux, C., Ruhle, S., Cahen, D., & Hodes, G. (2006). Chemical Bath Deposited Cds/Cdse-Sensitized Porous Tio2 Solar Cells. *Journal of Photochemistry and Photobiology a-Chemistry*, Vol. 181, No. 2-3, pp. 306-313, 1010-6030.

Nozik, A. J. (1976). P-N Photoelectrolysis Cells. *Applied Physics Letters*, Vol. 29, No. 3, pp. 150-153, 0003-6951.

Nozik, A. J. (2002). Quantum Dot Solar Cells. *Physica E-Low-Dimensional Systems & Nanostructures*, Vol. 14, No. 1-2, pp. 115-120, 1386-9477.

Ohko, Y., Tatsuma, T., Fujii, T., Naoi, K., Niwa, C., Kubota, Y., et al. (2003). Multicolour Photochromism of Tio2 Films Loaded with Silver Nanoparticles. *Nature Materials*, Vol. 2, No. 1, pp. 29-31, 1476-1122.

Oregan, B., & Gratzel, M. (1991). A Low-Cost, High-Efficiency Solar-Cell Based on Dye-Sensitized Colloidal Tio2 Films. *Nature*, Vol. 353, No. 6346, pp. 737-740, 0028-0836.

Oregan, B., & Schwartz, D. T. (1995). Efficient Photo-Hole Injection from Adsorbed Cyanine Dyes into Electrodeposited Copper(I) Thiocyanate Thin-Films. *Chemistry of Materials*, Vol. 7, No. 7, pp. 1349-1354, 0897-4756.

Park, H., Choi, W., & Hoffmann, M. R. (2008). Effects of the Preparation Method of the Ternary Cds/Tio2/Pt Hybrid Photocatalysts on Visible Light-Induced Hydrogen Production. *Journal of Materials Chemistry*, Vol. 18, No. 20, pp. 2379-2385, 0959-9428.

Paz, Y. (2011). Application of Tio2 Photocatalysis for Air Treatment: Patents' Overview. *Applied Catalysis B-Environmental*, Vol. 99, No. 3-4, pp. 448-460, 0926-3373.

Peng, T. Y., Dai, K., Yi, H. B., Ke, D. N., Cai, P., & Zan, L. (2008). Photosensitization of Different Ruthenium(Ii) Complex Dyes on Tio2 for Photocatalytic H-2 Evolution under Visible-Light. *Chemical Physics Letters*, Vol. 460, No. 1-3, pp. 216-219, 0009-2614.

Petit, M. A., & Plichon, V. (1996). Electrochemical Behavior of Wo3 Films in H3po4/H2o Binary Mixtures. *Journal of the Electrochemical Society*, Vol. 143, No. 9, pp. 2789-2794, 0013-4651.

Qiao, Q. Q., Xie, Y., & McLeskey, J. T. (2008). Organic/Inorganic Polymer Solar Cells Using a Buffer Layer from All-Water-Solution Processing. *Journal of Physical Chemistry C*, Vol. 112, No. 26, pp. 9912-9916, 1932-7447.

Quinn, R. K., Nasby, R. D., & Baughman, R. J. (1976). Photoassisted Electrolysis of Water Using Single-Crystal Alpha-Fe2o3 Anodes. *Materials Research Bulletin*, Vol. 11, No. 8, pp. 1011-1017, 0025-5408.

Ravelli, D., Dondi, D., Fagnoni, M., & Albini, A. (2009). Photocatalysis. A Multi-Faceted Concept for Green Chemistry. *Chemical Society Reviews*, Vol. 38, No. 7, pp. 1999-2011, 0306-0012.

Robel, I., Subramanian, V., Kuno, M., & Kamat, P. V. (2006). Quantum Dot Solar Cells. Harvesting Light Energy with Cdse Nanocrystals Molecularly Linked to

Mesoscopic Tio2 Films. *Journal of the American Chemical Society*, Vol. 128, No. 7, pp. 2385-2393, 0002-7863.

Ruhle, S., Shalom, M., & Zaban, A. (2010). Quantum-Dot-Sensitized Solar Cells. *Chemphyschem*, Vol. 11, No. 11, pp. 2290-2304, 1439-4235.

Santato, C., Ulmann, M., & Augustynski, J. (2001). Photoelectrochemical Properties of Nanostructured Tungsten Trioxide Films. *Journal of Physical Chemistry B*, Vol. 105, No. 5, pp. 936-940, 1089-5647.

Saremi-Yarahmadi, S., Wijayantha, K. G. U., Tahir, A. A., & Vaidhyanathan, B. (2009). Nanostructured Alpha-Fe2o3 Electrodes for Solar Driven Water Splitting: Effect of Doping Agents on Preparation and Performance. *Journal of Physical Chemistry C*, Vol. 113, No. 12, pp. 4768-4778, 1932-7447.

Saremi-Yarahmadi, S., Tahir, A. A., Vaidhyanathan, B., & Wijayantha, K. G. U. (2009). Fabrication of Nanostructured Alpha-Fe2o3 Electrodes Using Ferrocene for Solar Hydrogen Generation. *Materials Letters*, Vol. 63, No. 5, pp. 523-526, 0167-577X.

Sasaki, Y., Nemoto, H., Saito, K., & Kudo, A. (2009). Solar Water Splitting Using Powdered Photocatalysts Driven by Z-Schematic Interparticle Electron Transfer without an Electron Mediator. *Journal of Physical Chemistry C*, Vol. 113, No. 40, pp. 17536-17542, 1932-7447.

Sayama, K., Mukasa, K., Abe, R., Abe, Y., & Arakawa, H. (2001). Stoichiometric Water Splitting into H-2 and O-2 Using a Mixture of Two Different Photocatalysts and an Io3-/I- Shuttle Redox Mediator under Visible Light Irradiation. *Chemical Communications*, Vol. 23, pp. 2416-2417, 1359-7345.

Sayama, K., Mukasa, K., Abe, R., Abe, Y., & Arakawa, H. (2002). A New Photocatalytic Water Splitting System under Visible Light Irradiation Mimicking a Z-Scheme Mechanism in Photosynthesis. *Journal of Photochemistry and Photobiology a-Chemistry*, Vol. 148, No. 1-3, pp. 71-77, 1010-6030.

Scaife, D. E. (1980). Oxide Semiconductors in Photoelectrochemical Conversion of Solar-Energy. *Solar Energy*, Vol. 25, No. 1, pp. 41-54, 0038-092X.

Schaller, R. D., & Klimov, V. I. (2004). High Efficiency Carrier Multiplication in Pbse Nanocrystals: Implications for Solar Energy Conversion. *Physical Review Letters*, Vol. 92, No. 18, pp. 186601, 0031-9007.

Scharber, M. C., Wuhlbacher, D., Koppe, M., Denk, P., Waldauf, C., Heeger, A. J., et al. (2006). Design Rules for Donors in Bulk-Heterojunction Solar Cells - Towards 10 % Energy-Conversion Efficiency. *Advanced Materials*, Vol. 18, No. 6, pp. 789-+, 0935-9648.

Schurch, D., Currao, A., Sarkar, S., Hodes, G., & Calzaferri, G. (2002). The Silver Chloride Photoanode in Photoelectrochemical Water Splitting. *Journal of Physical Chemistry B*, Vol. 106, No. 49, pp. 12764-12775, 1520-6106.

Serpone, N., Borgarello, E., & Gratzel, M. (1984). Visible-Light Induced Generation of Hydrogen from H2s in Mixed Semiconductor Dispersions - Improved Efficiency through Inter-Particle Electron-Transfer. *Journal of the Chemical Society-Chemical Communications*, Vol. 6, pp. 342-344, 0022-4936.

Shalom, M., Dor, S., Ruhle, S., Grinis, L., & Zaban, A. (2009). Core/Cds Quantum Dot/Shell Mesoporous Solar Cells with Improved Stability and Efficiency Using an Amorphous Tio2 Coating. *Journal of Physical Chemistry C*, Vol. 113, No. 9, pp. 3895-3898, 1932-7447.

Shalom, M., Ruhle, S., Hod, I., Yahav, S., & Zaban, A. (2009). Energy Level Alignment in Cds Quantum Dot Sensitized Solar Cells Using Molecular Dipoles. *Journal of the American Chemical Society*, Vol. 131, No. 29, pp. 9876-9877, 0002-7863.

Shangguan, W. F. (2007). Hydrogen Evolution from Water Splitting on Nanocomposite Photocatalysts. *Science and Technology of Advanced Materials*, Vol. 8, No. 1-2, pp. 76-81, 1468-6996.

Shankar, K., Basham, J. I., Allam, N. K., Varghese, O. K., Mor, G. K., Feng, X. J., et al. (2009). Recent Advances in the Use of Tio2 Nanotube and Nanowire Arrays for Oxidative Photoelectrochemistry. *Journal of Physical Chemistry C*, Vol. 113, No. 16, pp. 6327-6359, 1932-7447.

Shen, Q., Kobayashi, J., Diguna, L. J., & Toyoda, T. (2008). Effect of Zns Coating on the Photovoltaic Properties of Cdse Quantum Dot-Sensitized Solar Cells. *Journal of Applied Physics*, Vol. 103, No. 8, pp, 0021-8979.

Shen, S. H., Guo, L. J., Chen, X. B., Ren, F., & Mao, S. S. (2010). Effect of Ag2s on Solar-Driven Photocatalytic Hydrogen Evolution of Nanostructured Cds. *International Journal of Hydrogen Energy*, Vol. 35, No. 13, pp. 7110-7115, 0360-3199.

Shin, W. S., Kim, S. C., Lee, S. J., Jeon, H. S., Kim, M. K., Naidu, B. V. K., et al. (2007). Synthesis and Photovoltaic Properties of a Low-Band-Gap Polymer Consisting of Alternating Thiophene and Benzothiadiazole Derivatives for Bulk-Heterojunction and Dye-Sensitized Solar Cells. *Journal of Polymer Science Part a-Polymer Chemistry*, Vol. 45, No. 8, pp. 1394-1402, 0887-624X.

Shinar, R., & Kennedy, J. H. (1982). Photoactivity of Doped Alpha-Fe2o3 Electrodes. *Solar Energy Materials*, Vol. 6, No. 3, pp. 323-335, 0165-1633.

Shockley, W., & Queisser, H. J. (1961). Detailed Balance Limit of Efficiency of P-N Junction Solar Cells. *Journal of Applied physics*, Vol. 32, No, pp. 510-519.

Siddiki, M. K., Li, J., Galipeau, D., & Qiao, Q. Q. (2010). A Review of Polymer Multijunction Solar Cells. *Energy & Environmental Science*, Vol. 3, No. 7, pp. 867-883, 1754-5692.

Sivula, K., Le Formal, F., & Gratzel, M. (2009). Wo3-Fe2o3 Photoanodes for Water Splitting: A Host Scaffold, Guest Absorber Approach. *Chemistry of Materials*, Vol. 21, No. 13, pp. 2862-2867, 0897-4756.

Solarska, R., Alexander, B. D., Braun, A., Jurczakowski, R., Fortunato, G., Stiefel, M., et al. (2010). Tailoring the Morphology of Wo3 Films with Substitutional Cation Doping: Effect on the Photoelectrochemical Properties. *Electrochimica Acta*, Vol. 55, No. 26, pp. 7780-7787, 0013-4686.

Subramanian, V., Wolf, E., & Kamat, P. V. (2001). Semiconductor-Metal Composite Nanostructures. To What Extent Do Metal Nanoparticles Improve the Photocatalytic Activity of Tio2 Films? *Journal of Physical Chemistry B*, Vol. 105, No. 46, pp. 11439-11446, 1089-5647.

Tada, H., Mitsui, T., Kiyonaga, T., Akita, T., & Tanaka, K. (2006). All-Solid-State Z-Scheme in Cds-Au-Tio2 Three-Component Nanojunction System. *Nature Materials*, Vol. 5, No. 10, pp. 782-786, 1476-1122.

Tak, Y., Hong, S. J., Lee, J. S., & Yong, K. (2009). Fabrication of Zno/Cds Core/Shell Nanowire Arrays for Efficient Solar Energy Conversion. *Journal of Materials Chemistry*, Vol. 19, No. 33, pp. 5945-5951, 0959-9428.

Takeda, Y., & Motohiro, T. Requisites to Realize High Conversion Efficiency of Solar Cells Utilizing Carrier Multiplication. *Solar Energy Materials and Solar Cells*, Vol. 94, No. 8, pp. 1399-1405, 0927-0248.

Tennakone, K., Kumara, G., Kottegoda, I. R. M., Wijayantha, K. G. U., & Perera, V. P. S. (1998). A Solid-State Photovoltaic Cell Sensitized with a Ruthenium Bipyridyl Complex. *Journal of Physics D-Applied Physics*, Vol. 31, No. 12, pp. 1492-1496, 0022-3727.

Thimsen, E., Le Formal, F., Gratzel, M., & Warren, S. C. (2011). Influence of Plasmonic Au Nanoparticles on the Photoactivity of Fe2o3 Electrodes for Water Splitting. *Nano Letters*, Vol. 11, No. 1, pp. 35-43, 1530-6984.

Tisdale, W. A., Williams, K. J., Timp, B. A., Norris, D. J., Aydil, E. S., & Zhu, X. Y. (2010). Hot-Electron Transfer from Semiconductor Nanocrystals. *Science*, Vol. 328, No. 5985, pp. 1543-1547, 0036-8075.

Tributsch, H., & Bennett, J. C. (1977). Electrochemistry and Photochemistry of Mos2 Layer Crystals .1. *Journal of Electroanalytical Chemistry*, Vol. 81, No. 1, pp. 97-111, 0022-0728.

Tsubomura, H., Matsumura, M., Nomura, Y., & Amamiya, T. (1976). Dye Sensitized Zinc-Oxide - Aqueous-Electrolyte - Platinum Photocell. *Nature*, Vol. 261, No. 5559, pp. 402-403, 0028-0836.

Tubtimtae, A., Wu, K. L., Tung, H. Y., Lee, M. W., & Wang, G. J. (2010). Ag2s Quantum Dot-Sensitized Solar Cells. *Electrochemistry Communications*, Vol. 12, No. 9, pp. 1158-1160, 1388-2481.

Turner, J. A. (1999). A Realizable Renewable Energy Future. *Science*, Vol. 285, No, pp. 687-689.

US_Department_of_Energy (2007). Technical Plan, Hydrogen Production, Multi-Year Research, Development and Demonstration Plan: Planned Program Activities for 2005-2015. Retrieved from http://www1.eere.energy.gov/hydrogenandfuelcells/mypp/index.html

US_Energy_Information_Administration (2010). International Energy Outlook 2010. Retrieved from http://www.eia.doe.gov/oiaf/ieo/pdf/0484(2010).pdf

van de Krol, R., Liang, Y. Q., & Schoonman, J. (2008). Solar Hydrogen Production with Nanostructured Metal Oxides. *Journal of Materials Chemistry*, Vol. 18, No. 20, pp. 2311-2320, 0959-9428.

Veziroglu, T. N., & Barbir, F. (1992). Hydrogen - the Wonder Fuel. *International Journal of Hydrogen Energy*, Vol. 17, No. 6, pp. 391-404, 0360-3199.

Walter, M. G., Warren, E. L., McKone, J. R., Boettcher, S. W., Mi, Q. X., Santori, E. A., et al. (2010). Solar Water Splitting Cells. *Chemical Reviews*, Vol. 110, No. 11, pp. 6446-6473, 0009-2665.

Wang, P., Zakeeruddin, S. M., Moser, J. E., & Gratzel, M. (2003). A New Ionic Liquid Electrolyte Enhances the Conversion Efficiency of Dye-Sensitized Solar Cells. *Journal of Physical Chemistry B*, Vol. 107, No. 48, pp. 13280-13285, 1520-6106.

Wang, P., Huang, B. B., Qin, X. Y., Zhang, X. Y., Dai, Y., Wei, J. Y., et al. (2008). Ag@Agcl: A Highly Efficient and Stable Photocatalyst Active under Visible Light. *Angewandte Chemie-International Edition*, Vol. 47, No. 41, pp. 7931-7933, 1433-7851.

Wang, X., Zhi, L. J., & Mullen, K. (2008). Transparent, Conductive Graphene Electrodes for Dye-Sensitized Solar Cells. *Nano Letters*, Vol. 8, No. 1, pp. 323-327, 1530-6984.

Weber, M. F., & Dignam, M. J. (1986). Splitting Water with Semiconducting Photoelectrodes Efficiency Considerations. *International Journal of Hydrogen Energy*, Vol. 11, No. 4, pp. 225-232, 0360-3199.

Wei, D. (2010). Dye Sensitized Solar Cells. *International Journal of Molecular Sciences*, Vol. 11, No. 3, pp. 1103-1113, 1422-0067.

Weinhardt, L., Blum, M., Bar, M., Heske, C., Cole, B., Marsen, B., et al. (2008). Electronic Surface Level Positions of Wo3 Thin Films for Photoelectrochemical Hydrogen Production. *Journal of Physical Chemistry C*, Vol. 112, No. 8, pp. 3078-3082, 1932-7447.

West, W. (1974). First Hundred Years of Spectral Sensitization. *Photographic Science and Engineering*, Vol. 18, No. 1, pp. 35-48, 0031-8760.

Wijayantha, K. G. U., Saremi-Yarahmadi, S., & Peter, L. M. (2011). Kinetics of Oxygen Evolution at Alpha-Fe2o3 Photoanodes: A Study by Photoelectrochemical Impedance Spectroscopy. *Physical Chemistry Chemical Physics*, Vol. 13, No. 12, pp. 5264-5270, 1463-9076.

Wilcoxon, J. P., & Samara, G. A. (1995). Strong Quantum-Size Effects in a Layered Semiconductor - Mos2 Nanoclusters. *Physical Review B*, Vol. 51, No. 11, pp. 7299-7302, 1098-0121.

Wu, T. X., Liu, G. M., Zhao, J. C., Hidaka, H., & Serpone, N. (1998). Photoassisted Degradation of Dye Pollutants. V. Self-Photosensitized Oxidative Transformation of Rhodamine B under Visible Light Irradiation in Aqueous Tio2 Dispersions. *Journal of Physical Chemistry B*, Vol. 102, No. 30, pp. 5845-5851, 1089-5647.

Wurfel, U., Peters, M., & Hinscht, A. (2008). Detailed Experimental and Theoretical Investigation of the Electron Transport in a Dye Solar Cell by Means of a Three-Electrode Configuration. *Journal of Physical Chemistry C*, Vol. 112, No. 5, pp. 1711-1720, 1932-7447.

Xu, L. X., Sang, L. X., Ma, C. F., Lu, Y. W., Wang, F., Li, Q. W., et al. (2006). Preparation of Mesoporous Invo4 Photocatalyst and Its Photocatalytic Performance for Water Splitting. *Chinese Journal of Catalysis*, Vol. 27, No. 2, pp. 100-102, 0253-9837.

Yan, H. J., Yang, J. H., Ma, G. J., Wu, G. P., Zong, X., Lei, Z. B., et al. (2009). Visible-Light-Driven Hydrogen Production with Extremely High Quantum Efficiency on Pt-Pds/Cds Photocatalyst. *Journal of Catalysis*, Vol. 266, No. 2, pp. 165-168, 0021-9517.

Ye, J. H., Zou, Z. G., Oshikiri, M., Matsushita, A., Shimoda, M., Imai, M., et al. (2002). A Novel Hydrogen-Evolving Photocatalyst Invo4 Active under Visible Light Irradiation. *Chemical Physics Letters*, Vol. 356, No. 3-4, pp. 221-226, 0009-2614.

Yin, L., & Ye, C. (2011). Review of Quantum Dot Deposition for Extremely Thin Absorber Solar Cells. *Science of advanced materials*, Vol. 3, No, pp. 41-58.

Yu, W. W., Qu, L. H., Guo, W. Z., & Peng, X. G. (2003). Experimental Determination of the Extinction Coefficient of Cdte, Cdse, and Cds Nanocrystals. *Chemistry of Materials*, Vol. 15, No. 14, pp. 2854-2860, 0897-4756.

Zhang, P., Kleiman-Shwarsctein, A., Hu, Y. S., Lefton, J., Sharma, S., Forman, A. J., et al. (2011). Oriented Ti Doped Hematite Thin Film as Active Photoanodes Synthesized by Facile Apcvd. *Energy & Environmental Science*, Vol. 4, No. 3, pp. 1020-1028, 1754-5692.

Zhang, Q. X., Guo, X. Z., Huang, X. M., Huang, S. Q., Li, D. M., Luo, Y. H., et al. (2011). Highly Efficient Cds/Cdse-Sensitized Solar Cells Controlled by the Structural

Properties of Compact Porous Tio2 Photoelectrodes. *Physical Chemistry Chemical Physics*, Vol. 13, No. 10, pp. 4659-4667, 1463-9076.

Zhao, D., Chen, C., Wang, Y., Ma, W., Zhao, J., Rajh, T., et al. (2008). Enhanced Photocatalytic Degradation of Dye Pollutants under Visible Irradiation on Al(Iii)-Modified Tio2: Structure, Interaction, and Interfacial Electron Transfer. *Environmental Science & Technology*, Vol. 42, No. 1, pp. 308-314, 0013-936X.

Zhao, W., Sun, Y. L., & Castellano, F. N. (2008). Visible-Light Induced Water Detoxification Catalyzed by Pt-Ii Dye Sensitized Titania. *Journal of the American Chemical Society*, Vol. 130, No. 38, pp. 12566-12567, 0002-7863.

Zong, X., Wu, G. P., Yan, H. J., Ma, G. J., Shi, J. Y., Wen, F. Y., et al. (2010). Photocatalytic H-2 Evolution on Mos2/Cds Catalysts under Visible Light Irradiation. *Journal of Physical Chemistry C*, Vol. 114, No. 4, pp. 1963-1968, 1932-7447.

Zou, Z. G., Ye, J. H., Sayama, K., & Arakawa, H. (2001). Direct Splitting of Water under Visible Light Irradiation with an Oxide Semiconductor Photocatalyst. *Nature*, Vol. 414, No. 6864, pp. 625-627, 0028-0836.

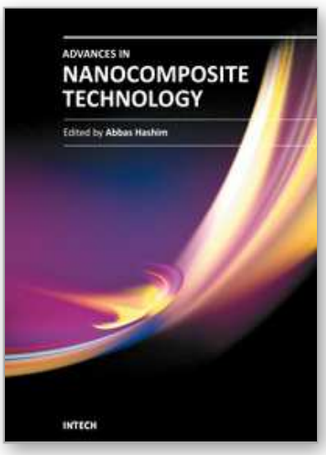

Advances in Nanocomposite Technology

Edited by Dr. Abbass Hashim

ISBN 978-953-307-347-7
Hard cover, 374 pages
Publisher InTech
Published online 27, July, 2011
Published in print edition July, 2011

The book â€œAdvances in Nanocomposite Technologyâ€ contains 16 chapters divided in three sections. Section one, â€œElectronic Applicationsâ€, deals with the preparation and characterization of nanocomposite materials for electronic applications and studies. In section two, â€œMaterial Nanocompositesâ€, the advanced research of polymer nanocomposite material and polymer-clay, ceramic, silicate glass-based nanocomposite and the functionality of graphene nanocomposites is presented. The â€œHuman and Bioapplicationsâ€ section is describing how nanostructures are synthesized and draw attention on wide variety of nanostructures available for biological research and treatment applications. We believe that this book offers broad examples of existing developments in nanocomposite technology research and an excellent introduction to nanoelectronics, nanomaterial applications and bionanocomposites.

INTECH
open science | open minds

InTech Europe
University Campus STeP Ri
Slavka Krautzeka 83/A
51000 Rijeka, Croatia
Phone: +385 (51) 770 447
Fax: +385 (51) 686 166
www.intechopen.com

InTech China
Unit 405, Office Block, Hotel Equatorial Shanghai
No.65, Yan An Road (West), Shanghai, 200040, China
中国上海市延安西路65号上海国际贵都大饭店办公楼405单元
Phone: +86-21-62489820
Fax: +86-21-62489821

IntechOpen